# Dalton Transactions

Accepted Manuscript






ROYAL SOCIETY OF CHEMISTRY

www.rsc.org/dalton

**Communicated to: Dalton Trans**
**Manuscript type : Article**
**MS ID: DT-ART-12-2014-003879 R1**



# Mixed Ligand Copper(II) Dicarboxylate Complexes: Role of Co-ligand Hydrophobicity on DNA Binding, Double-strand DNA Cleavage, Protein Binding and Cytotoxicity

Rangasamy Loganathan,[a] Sethu Ramakrishnan,[a] Mani Ganeshpandian,[a] Nattamai Bhuvanesh,[b] Mallayan Palaniandavar[a,c]* Anvarbatcha Riyasdeen,[d] and Mohamad Abdulkadhar Akbarsha[e,f]

[a]*School of Chemistry, Bharathidasan University, Tiruchirappalli – 620 024, Tamil Nadu, India*
[b]*X-ray Diffraction Lab, Department of Chemistry, Texas A&M University, College Station, TX 77842*
[c]*Department of Chemistry, Indian Institute of Technology Bombay, Mumbai 400 067, India*
[d]*Department of Animal Science, Bharathidasan University, Tiruchirappalli – 620 024, Tamil Nadu, India*
[e]*Mahatma Gandhi-Doerenkamp Center for Alternatives to use of Animals in Life Science Education, Bharathidasan University, Tiruchirappalli, 620024, Tamil Nadu, India*
[f]*Visiting Scientist, Department Food and Nutrition, King Saud University, Riyadh, Kingdom of Saudi Arabia*

*To whom correspondence should be addressed, e-mail: palanim51@yahoo.com and palaniandavarm@gmail.com

## Abstract

A few water soluble mixed ligand copper(II) complexes of the type [Cu(bimda)(diimine)] **1 - 5**, where bimda is *N*-benzyliminodiacetic acid and diimine is 2,2'-bipyridine (bpy, **1**) or 1,10-phenanthroline (phen, **2**) or 5,6-dimethyl-1,10-phenanthroline (5,6-dmp, **3**) or 3,4,7,8-tetramethyl-1,10-phenanthroline (3,4,7,8-tmp, **4**) and dipyrido[*3,2-d*: *2',3'-f*]quinoxaline (dpq, **5**), have been successfully isolated and characterized by elemental analysis and other spectral techniques. The coordination geometry around copper(II) in **2** is described as distorted square based pyramidal while that in **3** as square pyramidal. Absorption spectral titrations and competitive DNA binding studies reveal that the intrinsic DNA binding affinity of the complexes depends upon the diimine co-ligand, dpq (**5**) > 3,4,7,8-tmp (**4**) > 5,6-dmp (**3**) > phen (**2**) > bpy (**1**). The phen and dpq co-ligands are involved in π-stacking interaction with DNA base pairs while the 3,4,7,8-tmp/5,6-dmp and bpy co-ligands are involved in respectively hydrophobic and surface mode of binding with DNA. The small enhancement in relative viscosity of DNA upon binding to **1 - 5** supports the DNA binding modes proposed. Interestingly, **3** and **4** are selective in exhibiting a positive induced CD band (ICD) upon binding to DNA suggesting that they induce B to A conformational change. In contrast, **2** and **5** show CD responses which reveal their involvement in strong DNA binding. The complexes **2** - **4** are unique in displaying prominent double-strand DNA cleavage while **1** effects only single-strand DNA cleavage, and their ability to cleave DNA in the absence of an activator, varies as **5** > **4** > **3** > **2** > **1**. Also, all the complexes exhibit oxidative double-strand DNA cleavage activity in the presence of ascorbic acid, which varies as **5** > **4** > **3** > **2** > **1**. The ability of the complexes to bind and cleave the protein BSA varies in the order, **4** > **3** > **5** > **2** > **1**. Interestingly, **3** and **4** cleave the protein non-specifically in the presence of $H_2O_2$ as an activator suggesting that they can act also as chemical proteases. It is remarkable that **2** - **5** exhibit cytotoxicity against human breast cancer cell lines (MCF-7) with potency higher than the widely used drug cisplatin indicating that they have the potential to act as effective anticancer drugs in a time dependent manner. The morphological assessment data obtained by using Hoechst 33258 staining reveal that **3** and **4** induce apoptosis much more effectively than other complexes. Also, the alkaline single-cell gel electrophoresis study (comet assay) suggests that the same complexes induce DNA fragmentation more efficiently than others.

## Introduction

Cancer is one of the most dreadful and serious diseases in the world.[1] Cisplatin is the first metal-based drug currently used for the treatment of testicular and ovarian cancers while the "second generation drugs" such as carboplatin, and oxaliplatin are nowadays increasingly used in cancer treatment.[2,3] However, the platinum-based drugs are limited by side effects such as severe tissue toxicity including nephrotoxicity, ototoxicity, neurotoxicity, acquisition of resistance to the treatment, low water solubility and relative inactivity against gastrointestinal tumors.[4] So new non-platinum-based chemotherapeutics with novel mechanisms of action are being developed as alternative to platinum based drugs.[5] Numerous Cu(II), Ru(II), Fe(III), Co(III), Ni(II) and Zn(II) complexes have been investigated in search of new drugs with improved cytotoxicity. Copper complexes are considered[6,7] as the best promising alternatives to cisplatin as anticancer drugs because copper plays very important roles in several biological processes and many important enzymes rely on it for their catalytic activity.[8-10] Also, copper is important in angiogenesis,[11] which plays a key role in growth, development, and wound healing processes and, at the same time, it aids in tumor cell proliferation and metastasis.[12] The cytotoxicity of many synthetic copper(II) complexes have been investigated in recent years and particularly copper complexes containing 1,10-phenanthroline (phen) and related ligands have attracted much attention.[13-32]

Cisplatin is thought to engage in covalent binding to purine nucleobases of DNA forming intra- and interstrand DNA crosslinks and lead to cell death and severe side effects. So the focus is gradually shifting to non-covalently DNA binding copper(II) complexes so as to find complexes with improved pharmacological properties and broader range of antitumor activity. Very recently, we have found that the mixed ligand phenolate complexes of the type $[Cu(2NO)(phen)]^+$ are involved in non-covalent DNA binding while their corresponding chloride complexes [Cu(3N)Cl] are involved in covalent DNA interaction, and that the former complexes show higher DNA binding affinity, more efficient double strand DNA cleavage and higher cytotoxicity than the latter.[33] Also, certain mixed ligand μ-phenoxo-bridged dinuclear Cu(II) complexes with diimine co-ligands have been found to exhibit efficient chemical nuclease and protease activity and cytotoxicity.[34] Earlier also we have reported several mixed ligand copper(II) complexes of different primary ligands like iminodiacetic acid,[21] 2-[(2-(2-hydroxyethylamino)ethylimino)methyl]phenol (Htdp),[19] L-tyrosine,[20a] 2-hydroxy-*N*-(2-methylaminoethyl)benzamide[20b] and *N*,*N*-bis(benzimidazol-2-ylmethyl)amine (bba)[20c] with

diimine co-ligands. Most of these complexes strongly bind to DNA, cleave it effectively and exhibit prominent cytotoxicity more than cisplatin by inducing apoptosis. Some of the complexes of certain amino acids known as Casionpeínas® with phen-based co-ligands have received much attention due to their remarkable cytotoxicity with a significantly lower $IC_{50}$ value.[25] Kumbhar *et al.* developed certain mixed ligand Cu(II) diimine complexes of acetylacetone as cytotoxic agents.[26] Chen *et al.* isolated a few polypyridyl Cu(II) complexes along with the anticancer traditional Chinese medicine (TCM), plumbagin, which exhibit potent apoptotic activities.[27] Very recently, Trávníček *et al.* reported that the mixed ligand Cu(II) complexes of 3-hydroxy-4(1H)-quinolinone interact with DNA via partial intercalation, act as effective chemical nucleases and exhibit *in vitro* cytotoxicity.[28] Reedijk *et al.* have developed a completely new class of copper(II) anticancer complex of the type [Cu(phen)Cl(9Accm)], where 9Accm is the curcuminoid ligand 1,7-(di-9-anthracene-1,6-heptadiene-3,5-dione).[30] Pereira-Maia *et al.* have studied the cytotoxicity of the ternary copper(II) complexes $[Cu(dox)(phen)(H_2O)(ClO_4)](ClO_4)$ and $[Cu(tc)(phen)(H_2O)(ClO_4)](ClO_4)$, where dox is doxycycline and tc is tetracycline.[31]

In this report we have isolated a series of water soluble mixed ligand copper(II) complexes of the type [Cu(bimda)(diimine)] **1 - 5**, where bimda is *N*-benzyliminodiacetic acid and diimine is 2,2'-bipyridine (bpy, **1**) or 1,10-phenanthroline (phen, **2**) or 5,6-dimethyl-1,10-phenanthroline (5,6-dmp, **3**) or 3,4,7,8-tetramethyl-1,10-phenanthroline (3,4,7,8-tmp, **4**) and dipyrido[*3,2-d*: *2',3'-f*]quinoxaline (dpq, **5**) (**Scheme 1**), and explored the DNA binding and cleaving properties of the complexes to understand the effect of incorporating *N*-benzyl moiety on iminodiacetic acid upon the DNA binding affinity and double strand DNA cleavage activity of [Cu(imda)(diimine)] complexes,[21] which we have reported already, and hence the chemical principles underlying site-specific DNA recognition. It would be interesting to probe whether the enhanced hydrophobicity and steric bulk of *N*-benzyl moiety would affect the DNA binding and cleavage properties of the complexes and also improve their effectiveness as cytotoxic agents. The incorporation of dicarboxylic acid as the primary ligand may enhance the water solubility of the Cu(II) complexes and increase the cellular uptake leading to better cytotoxic drugs.[35,36] It is to be noted that the dicarboxylic acid derivatives of cisplatin such as carboplatin and oxaliplatin are more potent than cisplatin and Pt(II) complexes of *N*-substituted amino dicarboxylic acids show activity more potent than cisplatin and carboplatin.[37] The diimine co-ligands, apart from functioning as DNA recognition elements, may play a pivotal role in the mechanism underlying

induction of cell death by the mixed ligand complexes.[19,20] We have found that the hydrophobicity[38] of methyl groups of 3,4,7,8-tmp and 5,6-dmp co-ligands enhances the DNA binding affinity, and augments the chemotherapeutic activity of the complexes.

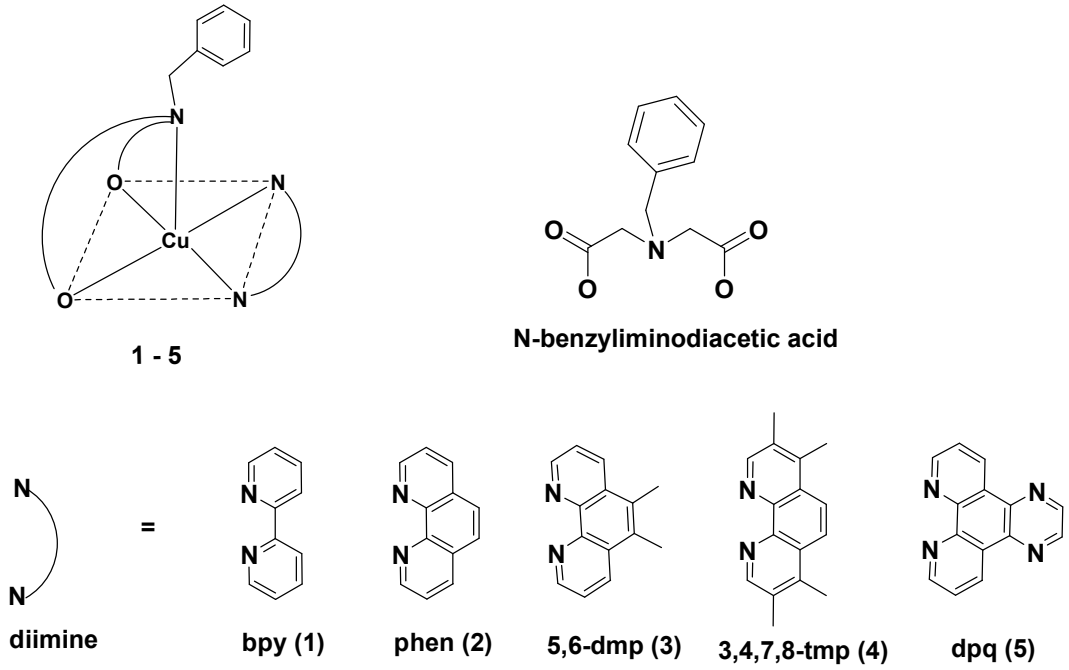


**Scheme 1** Schematic representation of copper(II) complexes **1** – **5** and the diimine co-ligands

Although there are other biological targets in tumor cells, including RNA, enzyme or protein, it is generally accepted that DNA is the primary target for many anticancer drugs[39] and almost all clinical agents, such as cisplatin and related platinum-based anticancer drugs active against aggressive cancers, act by binding covalently to the purine bases of DNA. So we have chosen to investigate the DNA binding properties of the complexes using calf thymus DNA. The complexes are found to be remarkable in bringing out efficient oxidative as well as hydrolytic double-strand cleavage of DNA in the absence of a reductant. This is interesting as double-strand DNA cleavage, among the various types of DNA cleavages, is of biological and therapeutic importance for greater cell lethality than single-strand cleavage because it appears to be less readily repaired by DNA repair mechanisms.[40] We have investigated the interaction of the complexes with the serum albumin BSA, which is the most abundant protein in blood plasma,[41] as the interaction between BSA and drugs determine the absorption, distribution, and metabolism of drugs.[42] We have chosen to screen the cytotoxicity of the DNA-cleaving copper(II) complexes

towards MCF 7 human breast cancer cell lines as breast cancer is the second most common cause of cancer-related death among women worldwide[43] and the currently used drug cisplatin is limited by its side effects. Interestingly, the complexes exhibit $IC_{50}$ values that are much lower than that of cisplatin for the same cell lines, indicating that they are promising drugs for cancer treatment. We have also explored whether the present DNA-targeted molecules are capable of triggering apoptosis[18,44] because tumor cells are more sensitive to apoptosis-inducing stimuli than normal cells.[45] It is remarkable that the complexes with 3,4,7,8-tmp and 5,6-dmp co-ligands kill the cancer cell lines through apoptosis more efficiently than the dpq complex and cisplatin. An important finding from this work is the very remarkable correlation made between the DNA double-strand cleavage efficiency and cytotoxicity of complexes.[46]

## Experimental section

### Synthesis of Ligand

The ligand dipyrido-[3,2-*d*:2',3'-*f*]-quinoxaline (dpq)[47] was prepared by reported procedure.

### Synthesis of Mixed Ligand Copper(II) Complexes

### Synthesis of [Cu(bimda)(bpy)] (1)

This complex was synthesized by adding to a methanol:water (4:1) solution of 2,2′-bipyridine (0.078 g, 0.5 mmol) and *N*-benzyliminodiacetic acid (0.112 g, 0.5 mmol), which was deprotonated by using a solution of NaOH (1 mmol equivalent), to a solution of copper(II) acetate (0.099 g, 0.5 mmol) in aqueous methanol solution (10 mL) and then stirring at 40 °C for 1 h. The resulting solution was filtered and kept aside for slow evaporation at room temperature. The blue crystalline solid that separated out was collected by suction filtration, washed with small amount of methanol, and then dried in vacuum. Anal Calcd for $C_{21}H_{19}CuN_3O_4$: C, 57.20; H, 4.34; N, 9.53; Found: C, 57.28; H, 4.44; N, 9.61. $\Lambda_M$ /$\Omega^{-1}$ cm$^2$ mol$^{-1}$: 9. $\lambda_{max}$/nm, 5 mM Tris-HCl / 50 mM NaCl buffer solution ($\varepsilon_{max}$/dm$^3$ mol$^{-1}$ cm$^{-1}$): 687(30), 298(9460). ESI-MS (MeCN) displays a peak at *m/z* 440.07 [Cu(bimda)(bpy)].

**Synthesis of [Cu(bimda)(phen)] ( 2)**

The complex was prepared by employing the procedure used for **1** and using 1,10-phenanthroline in the place of 2,2'-bipyridine. The blue needle-shaped crystals suitable for X-ray diffraction were obtained by slow evaporation of a concentrated solution of the complex. Anal Calcd for $C_{23}H_{19}CuN_3O_4$: C, 59.41; H, 4.12; N, 9.04; Found: C, 59.48; H, 4.23; N, 9.13. $\Lambda_M$ /$\Omega^{-1}$ $cm^2$ $mol^{-1}$: 7. $\lambda_{max}$/nm, 5 mM Tris-HCl / 50 mM NaCl buffer solution ($\varepsilon_{max}$/$dm^3$ $mol^{-1}$ $cm^{-1}$): 670(44), 272( 31290). ESI-MS (MeCN) displays a peak at *m/z* 464.07 [Cu(bimda)(phen)].

**Synthesis of [Cu(bimda)(5,6-dmp)] (3)**

The complex was prepared by using the procedure employed for **1** and using 5,6-dimethyl-1,10-phenanthroline in the place of 2,2'-bipyridine. The blue coloured crystals suitable for X-ray diffraction were obtained by slow evaporation of a concentrated solution of the complex. Anal Calcd for $C_{25}H_{23}CuN_3O_4$: C, 60.90; H, 4.70; N, 8.52; Found: C, 60.96; H, 4.83; N, 8.57. $\Lambda_M$ /$\Omega^{-1}$ $cm^2$ $mol^{-1}$: 9. $\lambda_{max}$/nm, 5 mM Tris-HCl / 50 mM NaCl buffer solution ($\varepsilon_{max}$/$dm^3$ $mol^{-1}$ $cm^{-1}$): 662(41), 278(19610). ESI-MS (MeCN) displays a peak at *m/z* 492.10 [Cu(bimda)(5,6-dmp)].

**Synthesis of [Cu(bimda)(3,4,7,8-tmp)] (4)**

The complex was prepared by employing the procedure employed for **1** and using 3,4,7,8-tetramethyl-1,10-phenanthroline in the place of 2,2'-bipyridine. The blue crystalline solid that separated out was collected by suction filtration, washed with small amount of methanol, and then dried in vacuum. Anal Calcd for $C_{27}H_{27}CuN_3O_4$: C, 62.24; H, 5.22; N, 8.06; Found: C, 62.36; H, 5.31; N, 8.17. $\Lambda_M$ /$\Omega^{-1}$ $cm^2$ $mol^{-1}$: 10. $\lambda_{max}$/nm, 5 mM Tris-HCl / 50 mM NaCl buffer solution ($\varepsilon_{max}$/$dm^3$ $mol^{-1}$ $cm^{-1}$): 667 (40), 279(16160). ESI-MS (MeCN) displays a peak at *m/z* 520.13 [Cu(bimda)(3,4,7,8-tmp)].

**Synthesis of [Cu(bimda)(dpq)] (5)**

The complex was prepared by adopting the procedure employed for **1** and using dipyrido-[3,2-*d*:2',3'-*f*]-quinoxaline in the place of 2,2'-bipyridine. Anal Calcd for $C_{25}H_{19}CuN_5O_4$: C, 58.08; H, 3.70; N, 13.55; Found: C, 58.16; H, 3.77; N, 13.59. $\Lambda_M$ /$\Omega^{-1}$ $cm^2$ $mol^{-1}$: 9. $\lambda_{max}$/nm, 5 mM Tris-HCl / 50 mM NaCl buffer solution ($\varepsilon_{max}$/$dm^3$ $mol^{-1}$ $cm^{-1}$): 674 (41), 251(24770). ESI-MS (MeCN) displays a peak at *m/z* 516.07 [Cu(bimda)(dpq)].

**Experimental Methods**

Microanalyses (C, H and N) were carried out with a Vario EL elemental analyzer. A Micro mass Quattro II triple quadrupole mass spectrometer was employed for ESI-MS analysis. UV-Vis spectra were recorded on a Shimadzu UV-Vis spectrophotometer using cuvettes of 1 cm path length. Emission intensity measurements were carried out by using a Jasco F 6500 spectrofluorimeter. Electron paramagnetic resonance (EPR) spectra for polycrystalline copper(II) complexes were obtained on a JEOL FA200 ESR spectrometer at room temperature. EPR spectra of the complexes in double distilled acetonitrile at liquid nitrogen temperature (77 K) were recorded on a JEOL JES-TE100 ESR spectrometer operating at X-band frequencies and having a 100 kHz field. 2,2'-diphenyl-l-picrylhydrazyl (DPPH) was used as the field marker. The viscosity measurements were carried out on a Schott Gerate AVS 310 automated viscometer thermostated at 25 $^{o}$C in a constant temperature bath. Circular dichroic spectra of DNA were obtained by using JASCO J-716 spectropolarimeter equipped with a Peltier temperature control device. Cyclic voltammetry and differential pulse voltammetry on a platinum sphere electrode were performed at 25.0 ± 0.2 $^{o}$C. The temperature of the electrochemical cell was maintained using a cryocirculator (HAAKE D8-G). Voltammograms were generated with the use of an EG&G PAR Model 273 potentiostat. A Pentium IV computer along with EG&G M270 software was employed to control the experiments and to acquire the data. A three-electrode system consisting of a platinum sphere (0.29 cm$^2$), a platinum auxiliary electrode and a reference electrode were used. The reference electrode for non-aqueous solution was Ag(s)/$Ag^+$, which consists of Ag wire immersed in a solution of $AgNO_3$ (0.01 M) and *tetra*-n-butylammonium perchlorate (0.1 M) in acetonitrile placed in a tube fitted with a vycor plug using a sleeve.[48] The cyclic voltammograms (CV) and differential pulse voltammograms (DPV) of copper(II) complexes were obtained in methanol solutions with *tetra-n*-butylammonium perchlorate as the supporting electrolyte at ambient temperatures under $N_2$. Redox potentials were measured relative to $Ag/Ag^+$ reference electrode. All the complexes are electroactive with respect to the metal center in the potential range ± 1.0 V. The redox potential ($E_{1/2}$) was calculated from the anodic ($E_{pa}$) and cathodic ($E_{pc}$) peak potentials of CV traces as ($E_{pa}$ + $E_{pc}$)/2 and also from the peak potential ($E_{pa}$) of DPV response as $E_p$ + $\Delta E$/2 ($\Delta E$ is the pulse height).

Solutions of DNA in the buffer 5 mM Tris-HCl / 50 mM NaCl buffer (pH = 7.2) in water gave the ratio of UV absorbance at 260 and 280 nm, $A_{260}/A_{280}$, of 1.9, indicating that the DNA

was sufficiently free of protein.[49] Concentrated stock solutions of DNA were prepared in a buffer and sonicated for 25 cycles, where each cycle consisted of 30 s with 1 min intervals. The concentration of DNA in nucleotide phosphate (NP) was determined by UV absorbance at 260 nm after 1:100 dilutions by taking the extinction coefficient, $\varepsilon_{260}$ as 6600 $M^{-1}$ $cm^{-1}$. Stock solutions of DNA were stored at 4 $^{o}$C and used after no more than 4 days. Supercoiled plasmid pUC19 DNA was stored at: -20 $^{\circ}$C and the concentration of DNA in base pairs were determined by UV absorbance at 260 nm after appropriate dilutions taking $\varepsilon_{260}$ as 13100 $M^{-1}$ $cm^{-1}$. Concentrated stock solutions of copper complexes were prepared by dissolving calculated amounts of the complexes in respective amounts of solvent and diluted suitably with the corresponding buffer to the required concentrations for all experiments. Synchronous fluorescence spectra of BSA with various concentrations of complexes were obtained from 300 to 400 nm when $\Delta\lambda$ = 60 nm and from 260 to 360 nm when $\Delta\lambda$ = 15 nm. The excitation and emission slit widths were 3 and 1.5 nm, respectively. Synchronous measurements were performed using a 1 cm quartz cell on a JASCO F 6500 spectrofluorimeter.

**X-Ray Crystallography**

The crystals of **2** and **3** of suitable size were selected from the mother liquor and, then mounted on the tip of a glass fiber and cemented using epoxy resin. Intensity data for both the crystals were collected using Mo-K$\alpha$ ($k$ = 0.71073 **Å**) radiation on a Bruker SMART Apex 2 diffractometer equipped with a CCD area detector at 150 K for **2** and at 293 K for **3** respectively. The SMART program[50] was used for collecting frames of data, indexing the reflections, and determining the lattice parameters. The data integration and reduction were processed with SAINT[51] software for **3**. Integrated intensity information for each reflection was obtained by reduction of the data frames with the program APEX2 for **2**.[50] The integration method employed a three dimensional profiling algorithm and all data were corrected for Lorentz and polarization factors, as well as for crystal decay effects. Finally the data was merged and scaled to produce a suitable data set. The absorption correction program SADABS[52] was employed to correct the data for absorption effects. The structures were solved by direct methods using SHELXTL (XS).[53] The structure was refined (weighted least squares refinement on $F^2$) to convergence.[54] All the non-hydrogen atoms in both the compounds were refined anisotropically till convergence is reached. Hydrogen atoms attached to the ligand moieties were stereochemically fixed. Absence

of additional symmetry and voids were confirmed using PLATON.[55] The crystallographic data and details of data collection for **2** and **3** (CCDC 1021461-1021462) are given in **Table 1**.

**DNA Binding and DNA Cleavage Experiments**

DNA binding and DNA cleavage studies were carried out by employing the procedure reported by us previously.[20]

## Tryptophan fluorescence quenching and protein cleavage studies

The tryptophan fluorescence quenching and protein cleavage studies were carried out as described previously.[56,57]

**Cell Culture**

The MCF 7 human breast cancer cell line was obtained from the National Center for Cell Science (NCCS), Pune, India. The cells were cultured in RPMI 1640 medium (Biochrom AG, Berlin, Germany) containing 10% fetal bovine serum (Sigma), 100 U/mL penicillin and 100 $\mu$g/mL streptomycin as antibiotics (Himedia, Mumbai, India) in 96-well culture plates at 37 °C under a humidified atmosphere of 2% $CO_2$ in a $CO_2$ incubator (Heraeus, Hanau, Germany). Cisplatin was purchased from Getwell pharmaceuticals, India. All experiments were performed using cells from passage 15 or less.

MTT assay, Hoechst 33258 Staining and Comet Assay were carried out as described previously.[20]

**Results and Discussion**

**Structures of Copper(II) Complexes in Solution**

The mixed ligand copper(II) complexes of the type [Cu(bimda)(diimine)] **1 - 5**, where bimda is *N*-benzyliminodiacetic acid and diimine is 2,2'-bipyridine (bpy, **1**) or 1,10-phenanthroline (phen, **2**) or 5,6-dimethyl-1,10-phenanthroline (5,6-dmp, **3**) or 3,4,7,8-tetramethyl-1,10-phenanthroline (3,4,7,8-tmp, **4**) and dipyrido[*3,2-d*: *2',3'-f*]quinoxaline (dpq, **5**), have been isolated. The formulas of the complexes [Cu(bimda)(diimine)] **1 – 5**, as determined by elemental analysis, are consistent with the X-ray crystal structures of **2** and **3**. In 5 mM Tris-HCl/50 mM NaCl buffer solution all the complexes exhibit only one broad band in the visible

region (660 – 690 nm) with very low absorptivity (**Table S1**), which is consistent with the square-based geometry observed in the solid-state structures of **2** and **3**. The intense absorption band observed in the UV region (250 - 300 nm) is attributed to the intraligand $\pi \rightarrow \pi^*$ transitions in the aromatic chromophores. The frozen solution EPR spectra of the complexes recorded in 5 mM Tris-HCl/50 mM NaCl buffer solution, display a copper hyperfine splitting pattern with the fourth line partially hidden in the $g_{x,y}$ region (**Figure S1**), which is typical of mononuclear Cu(II) (S = ½) complexes with essentially square-based geometry. Also, the observed EPR spectra of the complexes are axial with $g_{\|} > g_{\perp} > 2.0$ and $G^{58} = [(g_{\|} - 2)/(g_{\perp} - 2)] = 4.1 - 4.3$ confirming the square-based geometries diagnosed by electronic spectral measurements (**Table S2**). Further, a square-based $CuN_4$ chromophore is expected to show a $g_{\|}$ value of around 2.200 and an $A_{\|}$ value in the range 180 - 200 $\times 10^{-4}$ $cm^{-1}$ and replacement of a nitrogen atom in this chromophore by an oxygen atom is expected to increase the $g_{\|}$ value and decrease the $A_{\|}$ value.[59-60] On the other hand, distortion from square planar coordination geometry would increase the $g_{\|}$ value and decrease the $A_{\|}$ value. The observed $g_{\|}$ (2.252 - 2.258) and $A_{\|}$ (180 - 183 $\times$ $10^{-4}$ $cm^{-1}$) values are consistent with the presence of a square-based $CuN_2O_2$ chromophore with no significant distortion from planarity.[58] This is supported by the values of $g_{\|}/A_{\|}$ quotient, which fall within the range expected[20] for square planar geometry (123 – 125 cm). The ESI-MS data reveal that **1** - **5** display an essentially single mass peak assignable to mononuclear fragment [Cu(bimda)(diimine)] species, which is also supported by values of molar conductivity in methanol ($\Lambda_M$ /$\Omega^{-1}$ $cm^2$ $mol^{-1}$, 9 – 10) falling in the range[59c] for non-electrolytes. The cyclic (CV) and differential pulse voltammetric (DPV) responses obtained in methanol solution reveal that the Cu(II)/Cu(I) redox couple of **1 - 5** are far from reversible (**Table S3**, $E_{1/2}$, -0.085 to -0.185 V; $\Delta E_p$, 110 to 195 mV, **Figure S2**). The $E_{1/2}$ values vary as **5** > **4** > **3** < **2** > **1**, which reveals that dpq (**5**) stabilizes Cu(I) oxidation state more than phen (**2)** by involving in π-delocalization of electron density from copper more effectively and that the electron-releasing methyl groups on 5,6 (**3**) and 3,4,7,8 (**4**) positions stabilize Cu(II) state more than bpy (**1)**.

**Description of Structures of [Cu(bimda)(phen)]·2$H_2O$ (2) and [Cu(imda)(5,6-dmp)]·2.4$H_2O$ (3)**

The ORTEP representations of structures of **2** and **3** including atom numbering scheme are shown in **Figures 1** and **2** respectively and the crystal refinement data and selected bond lengths and bond angles are listed in **Table 2**. The copper atom in **2** and **3** is coordinated by two carboxylate oxygen (O1, O2) and the tertiary amine nitrogen (N3) atoms of the cis-facially coordinated bimda dianion and two nitrogen atoms (N1, N2) of phen (**2**)/5,6-dmp (**3**). The value of the structural index[61] τ of 0.29 [τ = (β- α)/60, where α = O3-Cu1-N2 = 155.20(9)° and β = O1-Cu1-N1 = 172.72 (9); for perfect square pyramidal and trigonal bipyramidal geometries the τ values are zero and unity,[62-64] respectively] for **2** reveals that the coordination geometry around copper(II) is best described as trigonal bipyramidal distorted square based pyramidal (TBDSBP)[62-64] with the corners of the $CuN_2O_2$ square plane occupied by N1 and N2 nitrogen atoms of phen and O1 and O3 oxygen atoms of bimda and the apical position occupied by N3 nitrogen atom of bimda. The tridentate ligand bimda is bound facially to Cu(II) with the two carboxylate oxygens (Cu-$O_{carboxylate}$, 1.928(2), 1.964(2) Å) located in the basal plane and the two imine nitrogens of phen (Cu-$N_{imine}$, 1.998(2), 2.003(2) Å) occupying the remaining corners of the basal plane. These bond distances are comparable to those found in $CuN_3O_2$ complexes with almost a similar geometry.[65-69] The strongly bound phen imine nitrogens occupy the equatorial sites around Cu(II) with the sterically hindered N3 amine nitrogen atom of bimda defaulting to the more weakly bound z-axial position (Cu(1)-N(3), 2.306(3) Å).[70] This is in contrast to the octahedral structure of [Cu(imda)(phen)($H_2O$)] in which the amine nitrogen of imda occupies the basal plane and one of the carboxylate oxygen atoms and the oxygen atom of water (O1W) occupy the axial positions.[21] The Cu-$N_{amine}$ bond is longer than the Cu-$N_{imine}$ bonds formed by phen, which is expected of $sp^3$ and $sp^2$ hybridizations respectively of amine and imine nitrogen atoms. The axial Cu-$N_{amine}$ bond is longer than the equatorial Cu-$N_{imine}$ bonds, which is expected of the presence of two electrons in the $d_{z^2}$ orbital of Cu(II). In the complex there is intramolecular π-π stacking interaction between the benzyl aromatic ring of coordinated bimda ligand and phen ring with the former being located approximately parallel to the coordination plane. Such stacking interactions have been reported earlier for the Cu(II) amino acid complexes [Cu(L-trp)(bpy)($H_2O$)]$^+$, [Cu(L-trp)(phen)]$^+$, [Cu(L-trp)(dppz)]$^+$, [Cu(L-tyr)(5,6-dmp)($H_2O$)]$^+$, [Cu(L-phe)(4,7-dmp)]$^+$ and [Cu(bzmal)(phen)($H_2O$)], where bzmal is benzylmalonic acid.[20,65-67,71] However, no such stacking interaction is observed for the imda complexes [Cu(NBIDA)(bpy)]$^+$,

[Cu(NBIDA)(phen)]$^+$, where NBIDA is *N*-(*p*-nitrobenzyl)iminodiacetic acid and [Cu(TEBIDA)(bpy)]$^+$, where TEBIDA is *N*-*tert*-butyliminodiacetic acid.[68,69]

The structure of **3** is similar to that of **2** with the tridentate ligand bimda bound facially to Cu(II) with the two carboxylate oxygens (Cu-$O_{carboxylate}$, 1.938(3), 1.929(3) Å) located in the basal plane and the two imine nitrogens of 5,6-dmp (Cu-$N_{imine}$, 1.996(3), 1.988(3) Å) occupying the remaining corners of the basal plane. However, the value of τ for **3** is 0.03 [τ = (β-α)/60, where α = O2-Cu1-N1 = 167.37(13) and β = O1-Cu1-N2 = 164.98(14)°] revealing that the coordination geometry around copper(II) is best described as square pyramidal[62-63] with no significant distortion toward trigonal bipyramidal geometry, and the lower τ value of **3** is due to stronger coordination of 5,6-dmp to Cu(II) (cf. below). Also, the τ value of **3** is lower than that (0.19) of the analogous complex [Cu(imda)(5,6-dmp)], which indicates that the benzyl substituents in the primary ligand leads to higher steric congestion at copper(II) in **3**. Upon replacing phen in **2** by 5,6-dmp to obtain **3**, the equatorial Cu–$N_{imine}$ bonds (Cu–N1, 1.996(3); Cu–N2, 1.988(3) Å) become shorter, which is expected of the stronger coordination of 5,6-dmp, negligible changes are observed in the Cu–$O_{carboxylate}$ bond distances and the axial Cu–$N3_{amine}$ (Cu–$N3_{imine}$, 2.302(3) Å) bond becomes slightly shorter. As in **2**, the sterically hindered N3 amine nitrogen atom of bimda defaults to the more weakly bound z-axial position, which is in contrast to [Cu(imda)(5,6-dmp)] in which the amine nitrogen occupies the equatorial position and one of the carboxylate oxygen atoms occupies the axial position.[23] Like **2**, the complex **3** also exhibits intramolecular π-π stacking with the distance between aromatic ring of bimda and the phen ring of 5,6-dmp being 3.497 Å.

**DNA Binding Studies**

**UV-Vis Absorption Spectral Titrations.** Upon the incremental addition of CT DNA to the complexes **1** – **5** the ligand centered π → π* absorption band (250 – 300 nm) shows increasing hypochromism (Δε, 17 - 48%) without any red-shift, suggesting groove binding preference of the complexes over intercalative mode of DNA binding (**Figure 3**). As the extent of hypochromism is commonly associated with the strength of DNA interaction,[20] the observed order of decrease in hypochromism, **5** > **4** ≈ **3** > **2** > **1**, reflects the decrease in DNA binding affinities of the complexes in this order. The DNA binding affinities of **1** – **5** are compared by obtaining the intrinsic DNA binding constant $K_b$ by using the equation described previously[34] (**Figure S3**). The

observed $K_b$ values (1.7 – 23.8 × $10^3$ $M^{-1}$, **Table 3**) are comparable to those reported for other mixed ligand copper(II) complexes with bidentate O,O donor ligands[26,27,31,71,72] and vary as **5** > **4** ≈ **3** > **2** > **1**, which is in conformity with the observed trend in hypochromism. They are lower than those observed[73] for the typical classical intercalator ethidium bromide (EthBr) ($K_b$, 4.94 × $10^5$ $M^{-1}$). Also, the $K_b$ values are significantly lower than those observed for the corresponding bis- and tris-diimine complexes namely, $[Cu(phen)_3]^{2+}$ ($K_b$, 9.8 × $10^3$ $M^{-1}$), $[Cu(5,6\text{-dmp})_3]^{2+}$ ($K_b$, 3.8 × $10^4$ $M^{-1}$),[74a] $[Cu(dpq)_2]^{2+}$ ($K_b$, 4.5 × $10^4$ $M^{-1}$),[29] $[Cu(dpq)_3]^{2+}$ ($K_b$, 7.5 × $10^4$ $M^{-1}$)[74a] and $[Cu(dppz)_2]^{2+}$ ($K_b$, 5.1 × $10^4$ $M^{-1}$)[29] but slightly higher than $[Cu(phen)_2]^{2+}$ ($K_b$, 2.7 × $10^3$ $M^{-1}$). Therefore, it is clear that the present complexes are involved in weaker DNA binding interactions obviously because they are neutral. The monocationic complexes [Cu(L-tyr)(diimine)]$^+$, [Cu(L-trp)(diimine)]$^+$, and [Cu(L-phe)(diimine)]$^+$, which are expected to display stronger DNA binding, show only moderate DNA binding affinities due to steric hindrance to DNA binding by the amino acid side chains.[71] Also, the observed $K_b$ values of **1** – **5** are higher than those ($K_b$, 0.60 – 17.0 × $10^3$ $M^{-1}$) of the corresponding [Cu(imda)(diimine)] complexes, illustrating that the hydrophobic benzyl group increases the DNA binding affinity and does not sterically hinder the DNA interaction. The hydrogen bonding interactions between the carboxylate oxygens with the functional groups positioned on the edge of DNA bases.[75] Similar hydrogen bonding interactions have been proposed for $[Co(NH_3)_6]^{3+}$ bound to $d(CG)_3$[76] and $[Ru(NH_3)_4(diimine)]^{2+}$ [77] bound to CT DNA. The DNA binding affinity of **5** is higher than that of **2**, the dpq co-ligand in the former is involved in π-stacking interaction with DNA stronger than the phen ring in the latter.[78] As **1** lacks a co-ligand with larger planar aromatic ring surface as in **2** and **5**, it is involved in weaker π-stacking interaction. The introduction of two and four methyl groups on phen ring in **3** and **4** respectively would sterically hinder the partial intercalation of phen ring with DNA base pairs. However, higher $K_b$ values are obtained for them suggesting a strong hydrophobic interaction between the methyl groups of 5,6-dmp and 3,4,7,8-tmp co-ligands in **3** and **4** and the hydrophobic interior accessible in DNA[19] rather than partial intercalation. Similar observations have been made by us earlier for the mononuclear complexes $[Cu(5,6\text{-dmp})_3]^{2+}$, $[Zn(5,6\text{-dmp})_3]^{2+}$ [74a] and $[Ru(5,6\text{-dmp})_3]^{2+}$,[74b] the mixed ligand complexes $[Ru(NH_3)_4(5,6\text{-dmp})]^{2+}$,[77] [Cu(imda)(5,6-dmp)],[21] $[Cu(dipica)(5,6\text{-dmp})]^{2+}$,[79] [Cu(tdp)(3,4,7,8-tmp)]$^+$,[19a] $[Cu(pmdt)(5,6\text{-dmp})]^{2+}$,[20d] $[Cu(bba)(5,6\text{-dmp})]^{2+}$ [20c] and $[Cu(L\text{-tyr})(5,6\text{-dmp})]^+$ [20a] and the dinuclear complexes $[\{(5,6\text{-dmp})_2Ru\}_2(bpm)]^{4+}$ [80] and $[Cu_2(LH)_2(5,6\text{-dmp})(ClO_4)_2]^{2+}$ [20b]

bound to CT DNA, all of them containing 5,6-dmp as the co-ligand, except [Cu(tdp)(3,4,7,8-tmp)]$^{2+}$. Upon increasing the number of methyl groups in phen ring from two in **3** to four in **4**, the DNA binding affinity increases. Thus, the π-stacking interaction of planar phen and dpq co-ligands and the hydrophobic interaction involving the methyl substituents on diimine co-ligands are the useful features for incorporation into Cu(II) complexes to optimize their DNA recognition.

**Ethidium Bromide Displacement Assay.** Upon adding **1 - 5** (0 – 60 μM) to CT DNA (125 μM) pretreated with ethidium bromide (EthBr, 12.5 μM) ([DNA]/[EthBr] = 10), only a slight decrease[81-83] in fluorescence intensity of EthBr is observed (**Figure S4**), revealing that they are not efficient in competing with the strong intercalator EthBr for the intercalative binding sites, and so the EthBr displacement mechanism is ruled out. The values of binding constant ($K_{app}$, **Table 3**) were calculated by using the method described previously.[34] Due to the steric hindrance of benzyl group **1** – **5** are involved in non-intercalative mode of DNA binding. If the quenching occurs by photoelectron transfer mechanism, then the ability of the complexes to quench the EthBr emission intensity should vary as **5** > **2** > **3** > **4** > **1**, depending upon the reducibility of the copper(II) complexes (cf. above), but the induced emission intensity of DNA-bound EthBr decreases in the order, **5** > **4** > **3** > **2** > **1**, which is consistent with the results from absorption spectral studies (**Table 3**, cf. above), and a plot of $K_b$ vs $K_{app}$ is linear (**Figure S5**). The highest $K_{app}$ value of **5** with the highest Cu(II)/Cu(I) redox potential (cf. below) reflects the facile electron-transfer from the excited state of EthBr to copper(II) (cf. above). Similarly, **2** with $E_{1/2}$ value higher than the 5,6-dmp (**3**) and 3,4,7,8-tmp analogues (**4**) would be expected to show a $K_{app}$ value higher than **3** and **4**. But the higher $K_{app}$ values observed for the latter indicate the predominant hydrophobic interaction of **3** and **4** with DNA.

**Viscosity Measurements.** Viscosity measurements were carried out on CT DNA with and without treating it with **1 - 5**. The values of relative specific viscosity ($\eta/\eta_0$), where $\eta$ and $\eta_0$ are the specific viscosities of DNA in the presence and absence of the complex respectively, are plotted against 1/R (= [Cu complex]/[DNA]) = 0 - 0.50 (**Figure S6**). The plot shows the ability of complexes to increase the viscosity of DNA depending upon the diimine co-ligand: dpq (**5**) ≥ 3,4,7,8-tmp (**4**) > 5,6-dmp (**3**) > phen (**2**) > bpy (**1**), which is consistent with the trends observed in values of $K_b$ and $K_{app}$ (cf. above). Though all the complexes show only minor changes in the

relative viscosity, the increase in viscosity observed for **5** is less than that for the classical intercalator EthBr but higher than that for **2** and also the minor groove binder Hoechst due to the π-stacking interaction of coordinated dpq (**5**), which is more intimate than that of phen ring (**2**). We have observed that [Cu(imda)(dpq)] shows $\Delta T_m$ value, and viscosity enhancement, higher than its phen and 5,6-dmp analogues, which is typical of partial intercalative interaction of coordinated dpq ligand. It is obvious that the strong hydrophobic interaction of coordinated 5,6-dmp and 3,4,7,8-tmp co-ligands with the interior of DNA grooves is also effective in increasing the length of DNA biopolymer.[19a] The complex **1** with non-planar bpy shows decrease in relative viscosity of CT DNA revealing weaker interaction of **1** to CT DNA. Thus, the results from viscosity measurements confirm the mode of DNA binding of the complexes established through absorption and emission spectral studies.

**Circular Dichroic Spectral Studies.** When **2**–**5** are incubated with DNA at 1/R = [Cu complex]/[DNA]) = 1, the CD spectrum of DNA undergoes interesting changes in both the positive and negative bands (**Figure 4**, **Table 3**).[84-85] The complexes **2** and **5** show a slight decrease and increase in band intensities of respectively the negative and positive bands indicating that the complexes perturb DNA helicity upon binding. Interestingly, the high-intensity bands for **2**, **3**, **4** and **5** superposed on the broad positive band at 273, 278, 279 and 298 nm, respectively, correspond to the positions of their UV absorption bands, and so they are induced CD (ICD) bands. Also, **3** and **4** show a higher red-shift (~14 nm) for both the bands with large increase and large decrease in intensities respectively of the positive (ICD) and negative bands, which originate from the effective placement of 5,6-dmp and 3,4,7,8-tmp chromophores with DNA grooves. This observation is consistent with B to A conformational change[19a,86] with the increased positive base pair tilting in A DNA caused by the hydrophobic interaction of 5,6-methyl groups with DNA. A similar red-shift (10 nm) observed for $[Cu(dipica)(5,6\text{-dmp})]^{2+}$ has been ascribed to B to A conformational change.[79]

**DNA Cleavage Studies**

**DNA Cleavage without Added Reductant.** As DNA cleavage activity is found to correlate with *in vitro* cytotoxicity of Cu(II) complexes,[15,20, 87,88] we have explored the DNA cleavage abilities of **1**–**5** by incubating them with supercoiled (SC) pUC19 DNA (40 μM) in the absence of an activator in 5 mM Tris-HCl/50 mM NaCl buffer at pH 7.1 for 1 h at 37 °C. All the complexes

effect double-strand DNA cleavage to generate the LC form before converting all of the SC form to NC form through single-strand break[21] (**Figure 5**) and the DNA cleavage efficiency follows the order **5** (80.6%) > **4** (78.8%) ≈ **3** (78.5%) ≈ **2** (76.5%) > **1** (70%), which is the same as that of DNA binding affinity (cf. above). Control experiments with ligand or $Cu(ClO_4)_2 \cdot 6H_2O$ or DNA alone do not reveal any cleavage. Interestingly, all the complexes effect double-strand DNA cleavage while [Cu(imda)(diimine)] complexes, except [Cu(imda)(dpq)], do not show any such cleavage,[21] illustrating that the *N*-benzyl moiety strongly perturbs the DNA molecule upon binding. The complex **5** shows higher cleavage ability, which is traced to its higher DNA binding affinity and Cu(II)/Cu(I) redox potential, while **3** and **4** show slightly higher DNA cleavage ability than **2** and **1**, possibly because of their enhanced hydrophobic interaction with DNA involving the co-ligands 5,6-dmp and 3,4,7,8-tmp. The effect of concentration of complexes on DNA cleavage rate was studied typically for **5** by using a constant concentration of SC pUC19 DNA (40 μM in base pair) under "pseudo-Michaelis-Menten" kinetic conditions with an incubation period of 60 min (**Figure 6**). The value of $K_{cat}$, which is the maximum rate of cleavage observed upon varying the catalyst concentration, is calculated[19a] as 0.49 (0.10 $h^{-1}$) under the present experimental conditions, and the corresponding value of $K_M$ is 77.2 μM. Though the cleavage rate enhancement is million fold in comparison with the uncatalyzed rate of cleavage of ds-DNA ($3.6 \times 10^{-8}$ $h^{-1}$),[89] it is comparable with those reported for transition metal-based synthetic hydrolases[89] and the observed value of the specificity constant ($K_{cat}/K_M$ ) $6.3 \times 10^3$ $h^{-1}$ $M^{-1}$ is lower than that ($4.8 \times 10^5$ $h^{-1}$ $M^{-1}$) for other mixed ligand Cu(II) complexes.[19,20,89] For **5**, the extent of DNA cleavage varies exponentially with incubation time and follows pseudo-first order kinetic profiles (**Figure S7**). The preliminary DNA strand scission mechanism of **5** has been investigated in the presence of hydroxyl radical scavenger (DMSO), the singlet oxygen quencher $NaN_3$, the superoxide scavenger SOD, the $H_2O_2$ scavenger catalase and under inert atmosphere (**Figure 7**). When the hydroxyl radical scavenger DMSO is added to the reaction mixture, inhibition of DNA cleavage is observed revealing that the cleavage reaction involves hydroxyl radicals. The addition of $NaN_3$ scarcely protects DNA against strand breakage induced by **5**, which suggests that neither $^1O_2$ nor any other singlet oxygen-like entity participates in the oxidative cleavage. This attenuation of the cleavage activity can be explained by taking into consideration reduction of Cu(II) species in the ROS production process. The catalase enzyme blocks the breakdown of DNA, revealing that hydrogen peroxide like species

may participate in the cleavage process. Furthermore, addition of superoxide dismutase (superoxide scavenger) to the reaction mixture does not show significant quenching of the cleavage reaction revealing that superoxide anion is not also the active species.[90] Thus the complexes **1- 5** are a few of the copper(II) complexes that are able to cleave DNA in the absence of a reducing agent under anaerobic conditions.

**DNA Cleavage with Ascorbic Acid Added as Reductant.** The DNA strand scission by **1 – 5** (30 μM) was studied in the presence of ascorbic acid (10 μM). In control experiments with DNA or ascorbic acid alone no DNA cleavage is observed. Interestingly, all the complexes convert the SC form to NC and LC forms, providing a clear evidence for direct double-strand DNA cleavage (**Figure 8**). The distribution of supercoiled, nicked and linear forms of DNA in the agarose gel electrophoresis provides a measure of the extent of DNA cleavage. The extent of DNA cleavage decreases in the order, **5** > **4 > 3 > 2 > 1** depending upon the co-ligand. The effect of concentration of the complexes on DNA cleavage was studied typically for **5** (which also shows the highest oxidative DNA cleavage activity) using a constant concentration of SC pUC19 DNA (40 μM in base pair). As the concentration of **5** is increased, the amount of form I (SC DNA) decreases and those of both forms II (NC DNA) and III (LC DNA) increase. The complex **5** exhibits efficient double-strand DNA cleavage, even at 5 μM concentration revealing that **5** behaves as an efficient chemical nuclease for double strand cleavage of DNA (**Figure 9**). The intense nuclease activity of **5** is apparently due to enhanced stabilization of the Cu(I) species formed, as evidenced by its highest Cu(II)/Cu(I) redox potential (cf. above). The ability of the dpq co-ligand with extended aromatic ring stabilizes Cu(I) oxidation state generated in the presence of ascorbic acid so that it is located close to the place of reaction by engaging in strong binding with DNA. The Cu(I) species binds to DNA with affinity higher than Cu(II) species[91] and thus DNA is made more accessible for the reactive oxygen species ($OH^{\cdot}$) produced by Fenton type reaction, resulting in higher DNA cleavage. So, it is obvious that strong DNA binding through π-stacking interactions is an important factor for efficient DNA cleavage. As the concentration of **4** is increased, the amount of form I decreases and those of both forms II and III increase and **4** also shows double-strand cleavage but at a slightly higher concentration (10 μM) revealing that **4** behaves as a chemical nuclease for oxidative double strand cleavage of DNA (**Figure 10**). The higher DNA cleavage activity of **4** is consistent with its enhanced hydrophobic

interaction with DNA. Similar conclusions have been made by us for $[Cu(tdp)(diimine)]^{+}$ complexes.[19a] Also, the 5,6-dmp complex exhibits better DNA cleavage activity due to its strong DNA binding affinity arising from hydrophobicity, like $[Cu(5,6\text{-dmp})_3]^{2+}$, $[Zn(5,6\text{-dmp})_3]^{2+}$ [74a] and $[Ru(5,6\text{-dmp})_3]^{2+}$,[74b] the mixed ligand complexes $[Ru(NH_3)_4(5,6\text{-dmp})]^{2+}$,[77] [Cu(imda)(5,6-dmp)],[21] $[Cu(dipica)(5,6\text{-dmp})]^{2+}$,[79] $[Cu(tdp)(3,4,7,8\text{-tmp})]^{+}$,[19a] $[Cu(pmdt)(5,6\text{-dmp})]^{2+}$ [20d] and $[Cu(L\text{-tyr})(5,6\text{-dmp})]^{+}$ [20a] and the dinuclear complexes $[\{(5,6\text{-dmp})_2Ru\}_2(bpm)]^{4+}$ [86] and $[Cu_2(LH)_2(5,6\text{-dmp})\text{-}(ClO_4)_2]^{2+}$.[20b] The lower DNA cleavage activity of **2** is consistent with its lower DNA binding affinity. The preliminary mechanism of DNA strand scission by **5** has been investigated in the presence of several additives under inert atmosphere. The results show that $^{\bullet}OH$ radicals rather than $^1O_2$ or $O_2^-$ or $H_2O_2$ are involved in the DNA cleavage reaction (**Figure 11**).

**Protein Binding and Cleavage Studies**

Though a very effective binding of a drug to serum albumin can be an unfavorable characteristic of a drug the study of molecular details of interaction of drugs with bovine serum albumin (BSA) could deepen the understanding and hence benefit the design of new antitumor complexes.[80] When **1**–**5** were treated with BSA, the emission intensity of BSA is found to decrease, revealing that the changes in the protein secondary structure as well as the tryptophan (trp-134, trp-212) environment of BSA occur upon binding of the complexes.[92] The extent of quenching of fluorescence intensity, as expressed by the value of Stern-Volmer constant ($K_{sv}$), is a measure of protein binding affinity of the complexes.[93] The value of $K_{sv}$, obtained as slope of the linear plot of $I_0/I$ *vs* [complex], follows the order **4** ≈ **3** > **5** > **2** > **1** (**Figure 12, Table 4**). The higher protein-binding affinity of **3** and **4** is due to the enhanced hydrophobicity provided by the methyl groups of 5,6-dmp and 3,4,7,8-tmp ligands. Synchronous fluorescence spectral study was used to obtain information about the molecular environment in the vicinity of the fluorophore moieties of BSA.[93] When the difference ($\Delta\lambda$) between the excitation and emission wavelengths is fixed at 15 and 60 nm, and the amount of **3** added to BSA (5 μM) is increased, a large decrease in fluorescence intensity with a small red-shift in the tryptophan emission maximum is observed. In contrast, the emission intensity of tyrosine residue is slightly decreased with no shift in the emission maximum (**Figure S8**). These observations confirm that the effective site of the fluorescence emission of BSA is the tryptophan residue. Also, the observed red-shift illustrates

that conformational changes occur near the hydrophobic tryptophan environment upon binding of **3** with increased hydrophobicity.

When the ability of **1 - 5** to cleave protein peptide bonds[94] was studied using BSA as substrate, the complexes are found to be ineffective (**Figure S9**). However, in the presence of $H_2O_2$ (500 μM), they show significant smearing or reduction in intensity of BSA bands (**Figure S10**) with respect to control (BSA alone without $H_2O_2$), suggesting that all the complexes are capable of cleaving the protein, but without any sequence specificity.

**Cytotoxicity Studies**

**MTT Assay**. The cytotoxicity of **2 – 5** against human breast cancer cell lines (MCF-7) was investigated in aqueous buffer solution[19,20] in comparison with the widely used drug cisplatin under identical conditions by using MTT assay. It was found that the $IC_{50}$ values for 48 h incubation are lower than those for 24 h incubation, clearly indicating that the observed cytotoxicity is time dependent. Interestingly, **2 - 5** exhibit cytotoxicity higher than cisplatin for both 24 and 48 h incubations and the potential of the complexes to kill cancer cells vary as **5 < 4 > 3 > 2** (**Table 5, Figure S11**). Also, **4** is remarkable in displaying cytotoxicity ($IC_{50}$, 2.5 (0.3) μM) approximately 10 times more prominent than cisplatin ($IC_{50}$, 24.5 (6.1) μM).[17] It is evident that the hydrophobic forces of interaction of **4** involving 3,4,7,8-tmp co-ligand leads to the highest cytotoxicity and, as expected, **3**, which is involved in hydrophobic interaction of 5,6-dmp co-ligand with both DNA and protein, displays a lower cytotoxicity ($IC_{50}$, 4.1 (0.6) μM). A similar correlation has been observed for the mixed ligand complexes $[Cu(tdp)(3,4,7,8\text{-tmp})]^{+}$,[19a] $[Cu(L\text{-tyr})(5,6\text{-dmp})]^{+}$,[20a] $[Cu(pmdt)(5,6\text{-dmp})]^{2+}$,[20d] $[Cu(bba)(5,6\text{-dmp})]^{2+}$ [20c] and $[Cu_2(LH)_2(5,6\text{-dmp})_2(ClO_4)_2]^{2+}$,[20b] which exhibit DNA binding affinity higher than their corresponding bpy, phen, and dpq analogues. Further, the enhanced hydrophobicity of 3,4,7,8-tmp **(4)** and 5,6-dmp **(3)** co-ligands facilitate transport of the complexes into the cell across cell membrane enabling them to interact with cellular DNA. The observed $IC_{50}$ values (2.5 – 11.3 μM, **Table 5**) are comparable to those reported for other mixed ligand copper(II) complexes with bidentate O,O donor ligands against MCF-7 breast cancer cell lines. The cytotoxicity of **2 - 5** are comparable to the mixed ligand copper(II) complexes $[Cu(acetylacetone)(diimine)]NO_3$ ($IC_{50}$ in 2.2 - 103.7 μM),[25] [Cu(plumbagin)(bpy)] ($IC_{50}$ in ~3.2 μM),[27] [Cu(2-phenyl-3-hydroxy-4(1H)-quinolinone)(diimine)]$NO_3$ ($IC_{50}$ in 1.0 - 27.2 μM),[28] [Cu(2-(naphthalen-1-yl)-1H-imidazo[4,5-

f][1,10]phenanthroline)(acac)]$NO_3$ ($IC_{50}$ in 1.2 - 3.2 μM),[26] [Cu(1,7-(di-9-anthracene-1,6-heptadiene-3,5-dione))(phen)Cl] ($IC_{50}$ in 4.0 - 61.0 μM),[30] and [Cu(moxifloxacin)(diimine)] ($IC_{50}$ in 16.7 - 18.1 μM).[95] As the cell killing activities of the present complexes are much higher than that of cisplatin,[96] they are suggested as suitable candidates for further study as potential applications as cytotoxic drugs.

**Hoechst Staining Studies**. Studies have supported that many antitumor agents used in chemotherapy are based on their ability to induce apoptosis in cancer cells.[97,98] So the molecular mechanism of cell death has been studied by treating the MCF 7 cancer cells with $IC_{50}$ concentrations of **3 - 5** for both 24 h and 48 h and then observing them for cytological changes by adopting Hoechst 33258 staining. The representative morphological changes observed for **3 - 5** such as chromatin fragmentation, bi- and/or multinucleation, cytoplasmic vacuolation, nuclear swelling, cytoplasmic blebbing and late apoptosis indication of dot-like chromatin condensation are shown in **Figure 13**. The number of abnormal cells is found to increase with incubation time revealing that all the complexes bring about cytological changes in a time dependent manner (**Figure 13**). Also, the number of abnormal cells generated at both 24 and 48 h varies as **4** > **3** > **5** (**Figure 13**). The higher apoptosis-inducing ability of **3** and **4** is consistent with the hydrophobicity of their diimine co-ligands, which facilitate transport of the complexes across the cell membrane and their eventual release at various organells in the cell leading to apoptosis. Similar observations have been made by us for the mixed ligand complexes [Cu(tdp)(3,4,7,8-tmp)]$^{+}$,[19a] [Cu(pmdt)(5,6-dmp)]$^{2+}$,[20d] [Cu(bba)(5,6-dmp)]$^{2+}$ [20c] and [Cu(L-tyr)(5,6-dmp)]$^{+}$ [20a] and the dinuclear complex [$Cu_2(LH)_2$(5,6-dmp)$(ClO_4)_2$]$^{2+}$ [20b] bound to CT DNA. As the apoptosis-inducing ability is critical in determining the efficacy of an anticancer drug, the complexes **3** and **4** with higher apoptosis-inducing ability are obviously more efficacious than **5**.

**Comet Assay**. The alkaline single cell gel electrophoresis or Comet assay provides an image of the changes that have occurred in the chromatin organization at a single cell level, which is considered a more accurate way of detecting early nuclear changes in a cell population.[99] When a cell with damaged DNA is subjected to electrophoresis and then stained with ethidium bromide (EthBr), it appears as a comet. Cells treated with **2 - 5** show statistically significant and well-formed comets, whereas the control (untreated) cells do not demonstrate any such comet like appearance (**Figure 14**). It is clearly seen that more than 50% of the damaged DNA is found in

the tail of the comet for **2** – **5**. Also, the longer tail length with highly intense comet like appearance observed for **4** and **5** is consistent with their highest cytotoxicity (cf. above) as the length of the comet tail is a measure of extent of DNA damage. This clearly indicates that **4** indeed induces higher DNA fragmentation, which is a further evidence for its ability to induce higher apoptosis. Also, the ability of **3** to degrade DNA is higher than that of **2**, which originates from its higher DNA binding affinity. The outcome of the Comet assay shows that DNA of a single cell undergoes degradation as a consequence of direct DNA damage or rapid apoptosis (evident from the nuclear staining) induced upon treatment with **4**. Apoptosis, unlike necrosis, induces minimal inflammatory responses and less toxic effects to the surrounding normal tissues and hence is more tolerable to patients.

All the above discussions clearly reveal that the prominent cytotoxicity of **3** and **4** is consistent with their high DNA binding affinities and also their high abilities to effect double-stranded DNA cleavage under physiological conditions and hence kill cancer cells. This supports our earlier finding[19-20] that ligand hydrophobicity plays a vital role in determining the cytotoxicity of a metal-based drug. The enhanced hydrophobicity of the complexes, apart from enhancing the DNA binding affinities, facilitates their transport into the cell (cf. above) so as to interfere with the cellular function of DNA. As the apoptosis-inducing ability is critical in determining the efficacy of an anticancer drug, **3** and **4** with apoptosis inducing ability higher than the other complexes, are more efficacious. However, additional biochemical experiments like cellular uptake, cell cycle analysis, mitochondrial membrane potential ($\Delta\Psi m$) to assess changes in the membrane potential, and Western blotting technique to evaluate the expression level of the pro- and antiapoptotic proteins are to be performed to confirm the modes of cell death observed for the complexes.

## Conclusions

Five water soluble mixed ligand complexes [Cu(bimda)(diimine)] have been isolated and studied. The coordination geometry around copper(II) in [Cu(bimda)(phen)] is described as distorted square-based pyramidal while that in [Cu(bimda)(5,6-dmp)] as square pyramidal. DNA binding experiments reveal that the intrinsic DNA binding affinity of the complexes depends upon the diimine co-ligand functioning as the DNA recognition element. The phen and dpq co-ligands are involved in π-stacking interaction with DNA base pairs while the 3,4,7,8-tmp or 5,6-dmp and bpy co-ligands are involved in respectively hydrophobic and electrostatic interactions

with DNA. Interestingly, the bpy complex exhibits only single-strand DNA cleavage while all the other complexes exhibit prominent double-strand DNA cleavage even in the absence of an activator. Also, all the complexes exhibit oxidative (ascorbic acid) double-strand DNA cleavage with the dpq and 3,4,7,8-tmp complexes being more robust and efficient. Further, the 5,6-dmp and 3,4,7,8-tmp complexes show protein (BSA) binding affinity higher than the other complexes, illustrating the importance of hydrophobic forces of interaction in protein binding. All the complexes cleave BSA non-specifically suggesting that they can act as chemical proteases. All the complexes, except bpy complex, exhibit cytotoxicity against human breast cancer cell line (MCF-7) with potency higher than the widely used drug cisplatin. The 5,6-dmp and 3,4,7,8-tmp complexes are remarkable in displaying cytotoxicity more potent than their dpq and phen analogues, which is consistent with their higher hydrophobicity and their higher ability to cleave DNA by double strand scission. Thus they are promising drugs for potential clinical applications in cancer therapy as they damage DNA by double strand cleavage and cause cell death mainly through apoptotic mode. So it is suggested that the diimine ligands 5,6-dmp and 3,4,7,8-tmp are incorporated as DNA as well as protein recognition elements in designing efficient metal-based anticancer agents. Further investigation on the complexes is needed to establish their ability to act as anti-cancer drugs.

**Supplementary material**

CCDC 1021461-1021462 contain the supplementary crystallographic data for this paper. These data can be obtained free of charge from the Cambridge Crystallographic Data Centre via http://www.ccdc.cam.ac.uk/data_request/cif.

**Acknowledgements**

We thank Department of Science and Technology (DST), New Delhi for Nano Mission Project (SR/NM/NS-110/2010 (G)) and Council of Scientific and Industrial Research (CSIR), New Delhi (CSIR/01(2462)/11/EMR-II) for financial support. The X-ray diffraction facility in Department of Chemistry, Bharathidasan University was created by funding from Department of Science and Technology (DST-FIST), New Delhi and EPR and fluorescence spectral facilities were created by funding from University Grants Commission (SAP), New Delhi. We thank Professor PR. Athappan, and Professor Ramu, Madurai Kamaraj University, Madurai for

providing the CD facilities, Dr. Balachandran Unni Nair, CLRI for providing the ESI-MS facilities and (late) Professor P. Sambasiva Rao, Pondicherry University for providing EPR facilities.

## REFERENCES


1. (a) J. Ferlay, H. R. Shin, F. Bray, D. Forman, C. Mathers and D. M. Parkin, International Agency for Research on Cancer; Lyon, France, 2008 (b) E. J. Gao, C. Liu, M. C. Zhu, H. K. Lin, Q. Wu and L. Liu, *Anti-Cancer Agents Med. Chem.* 2009, **9**, 356.

2. (a) G. AnnaRita, A. Maurizio, C. Claudio, G. Elisabetta and O. Domenico, *J. Inorg. Biochem.* 2004, **98**, 73; (b) E. Wong and C. M. Giandomenico, *Chem. Rev*. 1999, **99**, 2451; (c) T. Boulikas and M. Vougiouka, *Oncol. Rep.* 2003, **10**, 1663.

3. Y. W. Jung and S. J. Lippard, *Chem Rev*. 2007, **107***,* 1387–1407.

4. (a) A. M. Christiana, E. D. Constantinos and M. Christodoulos, *J. Inorg. Biochem.* 2008, **102**, 77; (b) R. T. Dorr and W. L. Fritz, *Cancer Chemotherapy Handbook, Henry Kimpton*, London, 1980; (c) A. H. Calvert, D. R. Newell and M. J. Tilby, *Cisplatin Nephrotoxicity, Oxford Textbook of Oncology*, Oxford University Press, Oxford, New York, 1995, **vol, 1**, p. 552; (d) G. Daugaard and U. Abildgaard, *Cisplatin nephrotoxicity,Cancer Chemother. Pharmacol,* 1989, **25**, 1; (e) M. J. Moroso, R. L. Blair, *J. Otolaryngol*, 1983, **12**, 36; (f ) L. X. Cubeddu, I. S. Hoffmann, N. T. Fuenmayor, A. L. Finn and N. Engl, *J. Med.Chem.* 1990, **322**, 810; (g) M. Kartalou and J. M. Essigmann, *Mutat. Res., Fundam. Mol. Mech. Mutagen.* 2001, **478**, 1; (h) L. R. Kelland, *Crit. Rev. Oncol. Hematol.* 1993, **15**, 191; (i) S. M. Cohen and S. J. Lippard, *Nucleic Acids Res. Mol. Biol.* **2001**, **67**, 93.

5. P. J. Bednarski, F. S. Mackay and P. J. Sadler, *Anticancer Agents Med. Chem.* **2007**, **7**, 75.

6. (a) X. Zhang, C. Bi, Y. Fan, Q. Cui, D. Chen, Y. Xiao and Q. Ping Dou, *Int. J. Mol. Med*., 2008, **22**, 677; (b) C. Marzano, M. Pellei, F. Tisano and C. Santini, *Anti-Cancer Agents Med. Chem*., 2009, **9**, 185; (c) S. Tardito and L. Marchio, *Curr. Med. Chem*., 2009, **16**, 1325.

7. (a) G. J. Brewer, *Exp. Biol. Med.,* 2001, **226**, 665; (b) T. Theophanides and J. Anastassopoulou, *Crit. Rev. Oncol. Hematol*., 2002, **42**, 57.

8. P. de Bie, P. Muller, C. Wijmenga and L.W. Klomp, *J. Med. Genet.* 2007, **44**, 673−688.

9. J. Lee, M. M. O. Pena, Y. Nose and D. J. Thiele, *J. Biol. Chem.* 2002, **277**, 4380−4387.

10. R. A. Pufahl, *Science* 1997, **278**, 853–856

11. L. Finney, S. Vogt, T. Fukai and D. Glesne, *Clin Exp Pharmacol Physiol.* 2009, **36**, 88–94

12. M. M. Eatock, A. Schatzlein and S. B. Kaye, *Cancer Treat Rev.* 2000, **26**, 191–204.

13. F. P. Dwyer, E. Mayhew, E. M. Roe and A. Shulman, *Br. J. Cancer*, 1965, **19**, 195.

14. X. Cai, N. Pan and G. Zou, *BioMetals*, 2007, **20(1)**, 1-11.

15. P. U. Maheswari, M. Ster, S. Smulders, S. Barends, G. P. Wezel, C. Massera, S. Roy, H. Dulk, P. Gamez and J. Reedijk, *Inorg. Chem.* 2008, **47**, 3719–3727.

16. D. Chen, V. Milacic, M. Frezza and Q. P. Dou, *Curr. Pharm. Des.* 2009, **15**, 777.

17. S. Tardito and L. Marchio, *Curr. Med. Chem.,* 2009, **16**, 1325.

18. Y. Jin and J. A. Cowan, *J. Am. Chem. Soc*. 2005, **127**, 8408–8415.

19. (a) V. Rajendiran, R. Karthik, M. Palaniandavar, H. S. Evans, V. S. Periasamy, M. A. Akbarsha, B. S. Srinag and H. Krishnamurthy, *Inorg.Chem.* 2007, **46**, 8208. (b) V. Rajendiran, M. Palaniandavar, P. Swaminathan and L. Uma, *Inorg.Chem.* (Commun) 2007, **46**, 8208.

20. (a) S. Ramakrishnan, V. Rajendiran, M. Palaniandavar, V. S. Periasamy, M. A. Akbarsha, B. S. Srinag and H. Krishnamurthy, *Inorg.Chem.* 2009, **48**, 1309. (b) S. Ramakrishnan, D. Shakthipriya, E. Suresh, V. S. Periasamy, M. A. Akbarsha and M. Palaniandavar, *Inorg.Chem.* 2011, **50**, 6458–6471. (c) R. Loganathan, S. Ramakrishnan, E. Suresh, A. Riyasdeen, M. A. Akbarsha and M. Palaniandavar, *Inorg. Chem.* 2011, **51**, 5512−5532. (d) M. Ganeshpandian, R. Loganathan, S. Ramakrishnan, A. Riyasdeen, M. A. Akbarsha and M. Palaniandavar, *Polyhedron* 2013, **52**, 929 – 938. (e) P. Jaividhya, R. Dhivya, M. A. Akbarsha and M. Palaniandavar, *J. Inorg. Biochem*. 2012, **94**, 105.

21. B. Selvakumar, V. Rajendiran, P. Uma Maheswari, H. S. Evans and M. Palaniandavar, *J. Inorg. Biochem.* 2006, **100**, 316–330.

22. J. D. Ranford, P. J. Sadler and D. A. Tocher, *J. Chem. Soc., Dalton Trans*., 1993, 3393–3399.

23. M. Scarpellini, A. Neves, R. Horner, A. J. Bortoluzzi, B. Szpoganicz, C. Zucco, R. A. N. Silva, V. Drago, A. S. Mangrich, W. A. Ortiz, A. C.W. Passos, M. C. B. Oliveira and H. Terenzi, *Inorg. Chem*., 2003, **42**, 8353–8365.

24. P. U. Maheswari, S. Roy, H. D. Dulk, S. Barends, G. V. Wezel, B. Kozlevcar, P. Gamez and J. Reedijk, *J. Am.Chem. Soc*., 2006, **128**, 710–711.

25. M. E. Bravo-Gómez, J. C. García-Ramos, I. Gracia-Mora and L. Ruiz-Azuara, *J. Inorg. Biochem.* 2009, **103**, 299 and references therein.

26. S. S. Bhat, A. A. Kumbhar, H. Heptullah, A. A. Khan, V. V. Gobre, S. P. Gejji and V. G. Puranik, *Inorg. Chem.* 2011, **50**, 545–558

27. Z. Chen, M. Tan, L. Liu, Y. Liu, H. Wang, B. Yang, A. Peng, H. Liu, H. Liang and C. Orvigd, *Dalton Trans.* 2009, 10824–10833

28. R. Buchtík, Z. Trávníček, J. Vančo, R. Herchel and Z. Dvořák, *Dalton Trans.* 2011, **40**, 9404–9412

29. B. Maity, M. Roy, S. Saha and A. R. Chakravarty, *Organometallics* 2009, **28**, 1495–1505. B. Maity, M. Roy, B. Banik, R. Majumdar, R. R. Dighe and A. R. Chakravarty, *Organometallics* 2010, **29**, 3632–3641. (c) T. K. Goswami, M. Roy, M. Nethaji, and A. R. Chakravarty, *Organometallics* 2009, **28**, 1992–1994. (d) B. Maity, M. Roy, and A. R. Chakravarty, *J. Organomet.Chem.* 2008, **693**, 1395–1399. (e) M. Roy, B. V. S. K. Chakravarthi, C. Jayabaskaran, A. Karande, and A. R. Chakravarty, *Dalton Trans*. 2011, **40**, 4855– 4864. (f) S. Dhar, D. Senapati, P. A. N. Reddy, P. K. Das, and A. R. Chakravarty, *Chem. Commun.* 2003, 2452–2453. (g) B. K. Santra, P. A. N. Reddy, G. Neelakanta, S. Mahadevan, M. Nethaji, and A. R. Chakravarty, *J. Inorg. Biochem*. 2002, **89**, 191. (h) T. Gupta, S. Dhar, M. Nethaji, and A. R. Chakravarty, *Dalton Trans.* 2004, **12**, 1896-1900.

30. N. Aliaga-Alcalde, P. Marqués-Gallego, V. Kraaijkamp, C. Herranz-Lancho, H. den Dulk, H. Görner, O. Roubeau, S. J. Teat, T. Weyhermüller, and J. Reedijk, *Inorg. Chem.* 2010, **49**, 9655–9663

31. P. P. Silva, W. Guerra, J. N. Silveira, A. M. C. Ferreira, T. Bortolotto, F. L. Fischer, H. Terenzi, A. Neves and E. C. Pereira- Maia, *Inorg. Chem.* 2011, **50**, 6414–6424.

32. S. Rajalakshmi, T. Weyhermüller, M. Dinesh and B. U. Nair, *J. Inorg. Biochem.* 2012, **117**, 48–59.

33. C. Rajarajeswari, M. Ganeshpandian, M. Palaniandavar, A. Riyasdeen and M. A. Akbarsha, *J. Inorg. Biochem.,* 2014, **140**, 255.

34. R. Loganathan, S. Ramakrishnan, E. Suresh, M. Palaniandavar, A. Riyasdeen and M.. A. Akbarsha, *Dalton Trans.,* 2014, **43**, 6177.

35. (a) E. Gao, L. Lin, L. Liu, M. Zhu, B. Wang and X. Gao, *Dalton Trans.* 2012, **41**, 11187 (b) E. Gao, M. Zhu, L. Liu, V. Huang, L. Wang, C. Shi, W. Zhang and Y. Sun, *Inorg. Chem.* 2010, **49**, 3261–3270

36. C. Deegan, M. McCann, M. Devereux, B. Coyle and D. A. Egan, *Cancer Letters* 2007, **247**, 224–233.

37. Y. Kim, R. Song, H. C. Chung, M. J. Jun and Y. S. Sohn, *J. Inorg. Biochem.* 2004, **98**, 98–104

38. P. U. Maheswari and M. Palaniandavar, *Inorg. Chim. Acta*. 2004, **357**, 901.

39. C. X. Zhang and S. J. Lippard, *Curr. Opin. Chem. Biol*. 2003, **7**, 481.

40. L. F. Povirk, In *Molecular Aspects of Anti-cancer Drug Action*; S. Neidle, M. Waring, Eds.; Verlag-Chemie: Weinheim, Germany, 1983; 157. (b) L. F. Povirk, *Mutat. Res.* 1991, **257**, 127.

41. F. Tian, F. Jiang, X. Han, C. Xiang, Y. Ge, J. Li, Y. Zhang, R. Li, X. Ding and Y. Liu. *J. Phys. Chem. B*. 2010**, 114***,* 14842–14853.

42. (a) F. Kratz, In *Metal Complexes in Cancer Chemotherapy*; B. K. Keppler, Ed.; VCH:Weinheim, Germany, 1993, 391. (b) M. J. McKeage, *Drug Safety* 1995, **13**, 228.

43. S. I. Khan, P. Aumsuwan, I. A. Khan,L. A. Walker and A. K. Dasmahapatra, *Chem. Res. Toxicol.* 2012, **25**, 61–73

44. F. Mancin, P. Scrimin, P. Tecilla and U. Tonellato, *Chem. Commun*. 2005, 2540–2548.

45. (a) U. Thatte and S. Dahanukar, *Drugs* 1997, **54**, 511–532. (b) J. Adams, *Drug Discov. Today,* 2003, **8**, 307–315.

46. P. P. Silva, W. Guerra, G. Coelho dos Santos, N. G. Fernandes, J. N. Silveira, A. M. da Costa Ferreira, T. Bortolotto, H. Terenzi, A. J. Bortoluzzi, A. Neves and E. C. Pereira-Maia, *J. Inorg. Biochem.* 2014, **132**, 67–76.

47. J. G. Collins, A. D. Sleeman, J. R. Aldrich, I. Greguric and T. W. Hambly, *Inorg. Chem.* 1998, **37**, 3133.

48. V. D. Parker, *in Electroanalytical Chemistry*, ed. A. J. Bard, Marcel Dekker, New York, 1986, vol. **14**, p. 18.

49. C. Merill, D. Goldman, S. A. Sedman and M. H. Ebert, *Science*, 1980, **211**, 1437–1438.

50. (a) SMART & SAINT Software References manuals, version 5.0, Bruker AXS Inc., Madison, WI, 1998. (b) APEX2 "Program for Data Collection on Area Detectors" BRUKER AXS Inc., 5465 East Cheryl Parkway, Madison, WI 53711-5373 USA

51. G. M. Sheldrick, SAINT 5.1, Siemens Industrial Automation Inc., Madison, WI, 1995.

52. SADABS, G. M. Sheldrick, "*Program for Absorption Correction of Area Detector Frames*", BRUKER AXS Inc., 5465 East Cheryl Parkway, Madison, WI 53711-5373 USA

53. G. M. Sheldrick, (2008). *Acta Cryst*. A64, 112-122. XS, BRUKER AXS Inc., 5465 East Cheryl Parkway, Madison, WI 53711-5373 USA.

54. O. V. Dolomanov, L. J. Bourhis, R. J. Gildea, J. A. K. Howard and H. Puschmann, "OLEX2: A Complete Structure Solution, Refinement and Analysis Program", *J. Appl. Cryst*. 2009, **42**, 339-341.

55. A. L. Spek, "PLATON - A Multipurpose Crystallographic Tool" *J. Appl. Cryst*. 2003, **36**, 7-13.; A. L. Spek, Utrecht University, Utrecht, The Netherlands 2008.

56. N. S. Quiming, R. B. Vergel, M. G. Nicolas and J. A. Villanueva, *J. Health Sci.* 2005, **51**, 8-15.

57. U. K. Laemmli, *Nature*, 1970, **227**, 680–685.

58. (a) B. J. Hathaway and D. E. Billing, *Coord. Chem. Rev.* 1970, **5**, 143-207. (b) U. Sakaguchi and A. W. Addison, *J. Chem.Soc. Dalton Trans.* 1979, 600.

59. (a) U. Sakaguchi and A. W. Addison, *J. Chem.Soc. Dalton*, 1979, 600. (b) M. Palaniandavar, I. Somasundaram, M. Lakshminarayanan and H. Manohar, *Dalton Trans.* 1996, 1333–1340. (c) J. E. Huheey, E. A. Keiter, R. L. Keiter and O. K. Medhu, *Inorganic Chemistry, Principles of Structure and Reactivity*; Pearson Education: Upper Saddle River, NJ, 2006, 425-426.

60. (a) J. Peisach and W. E. Blumberg, *Archi of Biochem and Biophy,* 1974, **165**, 691-708 (b) M. Murali, M. Palaniandavar and T. Pandiyan, *Inorg. Chim. Acta.* 1994, **224**, 19.

61. (a) A. W. Addison, T. N. Rao, J. Reedijk, J. V. Rijn and G. C. Verschoor, *J. Chem. Soc., Dalton Trans.,* 1984, 1349-1356. (b) G. Murphy, P. Nagle, B. Murphy and B. Hathway, *Dalton Trans.* 1997, 2645–2652.

62. G. Murphy, C. Murphy, B. Murphy and B. Hathway, *Dalton Trans.* 1997, 2653–2660.

63. P. Nagle, E. O'Sullivan and B. Hathway, *J. Chem. Soc., Dalton Trans.* 1990, 3399–3406.

64. P. Tamil Selvi, M. Murali, M. Palaniandavar, M. Kockerling and G. Henkel, *Inorg.Chim. Acta B*. 2002, **340**, 139–146.

65. (a) T. K. Goswami, S. Gadadhar, A. A. Karande and A. R. Chakravarty, *Polyhedron* 2013, **52**, 1287-1298 , (b) T. K. Goswami, V. S. K. Balabhadrapatruni, C. M. Roy, A. A. Karande and A. R. Chakravarty, *Inorg. Chem,* 2011, **50**, 8452

66. C. Sua, T. Taia, S. Wua, S. Wang and F. Liao, *Polyhedron* 1999, **18**, 2361–2368

67. A. Castiñeiras, A. G. Sicilia-Zafra, J. M. González-Pérez, D. Choquesillo-Lazarte and J. Niclós-Gutiérrez, *Inorg. Chem*. 2002, **41**, 6956–6958.

68. M. J. Sánchez-Moreno, D. Choquesillo-Lazarte, J. M. González-Pérez, V. Carballo, J. D. Martín-Ramos, A. Castiñeiras and J. Niclós-Gutiérrez, *Polyhedron* 2003, **22**, 1039-1049.

69. P. X. Rojas-González, D. Choquesillo-Lazarte, J. M. González-Pérez, S. A. Ruíz-García, R. Carballo, A. Castiñeiras and J. Niclós-Gutiérrez, *Polyhedron* 2003, **22**, 1027-1037

70. (a) M. Palaniandavar, T. Pandiyan, M. Lakshminarayanan and H. Manohar, *J. Chem. Soc., Dalton Trans.* 1995, **3**, 455. (b) K. Pijus, S. Sasmal Saha, R. Majumdar, R. R. Dighe and A. R. Chakravarty, *Inorg. Chem.* 2010, **49**, 849–859 (c) J. Liu, Z. Song, L. Wang, J. Zhuang, X. You and X. Huang, *Transition Met. Chem.* 1999, **24**, 499.

71. A. K. Patra, T. Bhowmick, S. Ramakumar, M. Nethaji and A. R. Chakravarty, *Dalton Trans.* 2008, 6966–6976

72. R. Singh, R. N. Jadeja, M. C. Thounaojam, T. Patel, R. V. Devkar and D. Chakraborty, *Inorg. Chem. Commun*. 2012, **23***,* 78–84.

73. V. A. Bloomfield, D. M. Crothers and I. Tinocco, *Jr., Physical Chemistry of Nucleic Acids, Harper & Row,* New York, **1974**, p. 432.

74. (a) S. Ramakrishnan and M. Palaniandavar, *Dalton Trans*. 2008, 3866. (b) P. U. Maheswari, V. Rajendiran, H. S. Evans and M. Palaniandavar, *Inorg.Chem.* 2006, 45, 37.

75. H. L. Chan, H. Q. Liu, B. C. Tzeng, Y. S. You, S. M. Peng, M. Yang and C. M. Che, *Inorg. Chem.* 2002, **41**, 3161.

76. V. Boom and A. Rich, *Biochemistry* 1985, **24**, 237.

77. P. U. Maheswari and M. Palaniandavar, *J. Inorg.* Biochem. 2004, **98**, 219.

78. A. Natrajan and S. M. Hecht, In *Molecular Aspects of Anticancer Drug- DNA Interactions;* S. Neidle, M. Waring, Eds.; CRC Press: Boca Raton, FL, 1994, **2**, 197.

79. S. Ramakrishnan and M. Palaniandavar, *J. Chem. Sci.* 2005, 117, 179.

80. S. D. Cummings, *Coord. Chem. Rev*. 2009, **253***,* 1495-1516

81. F. J. Meyer-Almes and D. Porschke, *Biochemistry* 1993, **32**, 4246–4253.

82. G. M. Howe, K. C. Wu and W. R. Bauer, *Biochemistry* 1976, **19**, 339–347.

83. S. Satyanarayana, J. C. Dabrowiak and J. B. Chaires, *Biochemistry* 1992, **31***,* 9319-9324.

84. M. Asadi, E. Safaei, B. Ranjbar and L. Hasani, *J. Mol. Struct.* 2005, **754**, 116–123.

85. G. Cervantes, M. J. Prieto and V. Moreno, *Metal Based Drug* 1997, **54**, 49–18.

86. P. U. Maheswari, V. Rajendiran, R. Parthasarathi, V. Subramanian and M. Palaniandavar, *Bull. Chem. Soc. Jpn.* 2005, **78**, 835.

87. (a) P. U. Maheswari, M. V. D. Ster, S. Smulders, Barends, G. P. V. Wezel, C. Massera, S. Roy, H. D. Dulk, P. Gamez and J. Reedijk, J. *Inorg. Chem*. 2008, **47**, 9. (b) F. M. Muggia, T. Fojo, *J. Chemotherapy* 2004, **4**, 77. (c) P. Falco, S. Bringhen, I. Avonto, F. Gay, F. Morabito, M. Boccadoro and A. Palumbo, *Expert Rev. Anticancer Ther.* 2007, **7**, 945. (d) D. Catovsky, M. Else and S. Richards, *Clin. Lymphoma Myeloma Leuk.* 2011, **11**, S2. (e) M. Froudarakis, E. Hatzimichael, L. Kyriazopoulou, K. Lagos, P. Pappas, A. Tzakos, V. Karavasilis, D. Daliani, C. Papandreou and E. Briasoulis, *Crit. Rev. Oncol. Hematol.* 2013, **87**, 90–100.

88. A. Sreedhara, J. D. Freed and J. A. Cowan, *J. Am. Chem. Soc.* 2000, **122**, 8814-8824.

89. J. Wang, Q. Xia, X. Zheng, H. Chen, H. Chao, Z. Mao and L. N. Ji, *Dalton Trans.,* 2010, **39**, 2128–2136.

90. E. Lamour, S. Routier, J. L. Bernier, J. P. Catteau, C. Bailly and H. Vezin, *J. Am, Chem.Soc.* 1999, **121***,* 1862-1869.

91. S. Mahadevan and M. Palaniandavar, *Inorg. Chem*., 1998, **37**, 3927-3934.

92. T. Peters, *Adv. Protein Chem*. 1985, **37**, 161.

93. (a) J. R. Lakowicz, *Principles of Fluorescence Spectroscopy*, 2nd ed.; Plenum Press: New York, 1999. (b) N. Wang, L. Ye, B.Q. Zhao, J.X. Yu, and Braz. *J. Med. biol. Res.* 2008, **41**, 589-595.

94. T. N. Parac and N. M. Kostic´, *J. Am. Chem. Soc.* 1996, **118***,* 51-58.

95. S. Patitungkho, S. Adsule, P. Dandawate, S. Padhye, A. Ahmad and F. H. Sarkar, *Bioorg. Med. Chem. Lett.* 2011, **21***,* 1802–1806

96. S. Komeda, M. Lutz, A. L. Spek, M. Chikuma and J. Reedijk, *Inorg. Chem*. 2000, **39**, 4230.

97. S. Komeda, M. Lutz, A. L. Spek, Y. Yamanaka, T. Sato, M. Chikuma, and J. Reedijk, *J. Am, Chem. Soc.* 2002, **124**, 4738.

98. I. M. Ghobrial, T. E. Witzig and A. A. Adjei, *Ca-Cancer J. Clin.* 2005, **55**, 178.

99. C. Alapetite, T. Wachter, E. Sage and E. Moustacchi, *Int. J. Radiat. Biol.* 1996, **69**, 359.

**Table 1.** Crystal data and structure refinement details for **2** and **3**

| | **2** | **3** |
|---|---|---|
| Empirical formula | $C_{23}H_{23}CuN_3O_6$ | $C_{25}H_{23}CuN_3O_4 \cdot 2.4(H_2O)$ |
| Formula weight | 500.98 | 536.24 |
| Crystal system | Monoclinic | Monoclinic |
| Space group | P2(1)/c | C 1 2/c 1 |
| a, Å | 9.873(3) | 25.6146(17) |
| b, Å | 16.336(5) | 12.8338(7) |
| c, Å | 13.048(4) | 18.1002(12) |
| α, deg | 90 | 90 |
| β, deg | 99.869(4) | 124.050(5) |
| γ, deg | 90 | 90 |
| V, Å$^3$ | 2073.3(11) | 4930.0(6) |
| Z | 4 | 8 |
| λ, Å | MoKα, 0.71073 | MoKα, 0.71073 |
| $D_{calc,}$ g.cm$^{-3}$ | 1.605 | 1.445 |
| Goodness-of-fit on $F^2$ | 1.097 | 1.078 |
| Number of reflections used | 4729 | 3870 |
| Number of refined Parameters | 298 | 337 |
| Final R indices [I>2 σ(I)] | | |
| [a]R1 | 0.0489 | 0.0478 |
| [b]wR2 | 0.1313 [a] | 0.1357[a] |

[a] $R1 = [\Sigma(||Fo|-|Fc||)/\Sigma|Fo|]$ [b] $wR2 = \{[\Sigma(w(Fo^2-Fc^2)^2)/\Sigma(wFo^4)]^{1/2}\}$

**Table 2.** Selected bond lengths [Å] and angles [deg] for **2** and **3**

| Bond Lengths [Å] | **2** | **3** |
|---|---|---|
| Cu1-O1 | 1.928(2) | 1.929(3) |
| Cu1-O2 | 1.964(2) | 1.938(3) |
| Cu1-N2 | 1.998(2) | 1.988(3) |
| Cu1-N1 | 2.003(2) | 1.996(3) |
| Cu1-N3 | 2.306(3) | 2.302(3) |
| Angles [deg] | | |
| O1-Cu1-O2 | 91.73(10) | 91.29(16) |
| O1-Cu1-N2 | 172.72(9) | 164.98(14) |
| O1-Cu1-N1 | 90.93(10) | 92.56(14) |
| O1-Cu1-N3 | 82.48(9) | 81.55(13) |
| O2-Cu1-N2 | 93.52(10) | 91.63(14) |
| O2-Cu1-N1 | 155.20(9) | 167.37(13) |
| O2-Cu1-N3 | 80.84(9) | 81.15(13) |
| N1-Cu1-N2 | 82.20(10) | 81.65(12) |
| N2-Cu1-N3 | 103.33(9) | 113.46(12) |
| N1-Cu1-N3 | 123.95(9) | 111.32(13) |

**Table 3.** Ligand-based absorption spectral properties[a], fluorescence spectral properties[b] and CD spectral parameters[c] of copper(II) complexes bound to CT DNA

| Complex | $\lambda_{max}$ (nm) | R | Change in Absorbance | Δε (%) | $^{a}K_b$ ($\times 10^3$ $M^{-1}$) | $^{b}K_{app}$ ($\times 10^4$ $M^{-1}$) | [c]Wavelength (nm) | |
|---|---|---|---|---|---|---|---|---|
| DNA | - | - | - | - | - | - | 246 | 276 |
| [Cu(bimda)(bpy)] **1** | 298 | 25 | Hypochromism | 17 | 1.7 ± 0.1 | 1.3 | - | - |
| [Cu(bimda)(phen)] **2** | 272 | 25 | Hypochromism | 42 | 4.3 ± 0.4 | 3.6 | 246 | 280 |
| [Cu(bimda)(5,6-dmp)] **3** | 278 | 25 | Hypochromism | 45 | 5.9 ± 0.3 | 3.8 | 248 | 289 |
| [Cu(bimda)(3,4,7,8-tmp)] **4** | 279 | 25 | Hypochromism | 44 | 6.0 ± 0.5 | 4.2 | 256 | 290 |
| [Cu(bimda)(dpq)] **5** | 251 | 25 | Hypochromism | 48 | 23.8 ± 0.9 | 14.0 | 245 | 270 |

[a]Measurements were made at R = 25, where R = [DNA]/[complex], concentration of solutions of copper(II) complexes = $30 \times 10^{-6}$ M (**2** and **3** ) $20\times 10^{-6}$ M (**4, 5**) and $40\times 10^{-6}$ M (**1**).
[b]Apparent DNA binding constant from ethidium bromide displacement assay using increasing concentration (0 - 60 μM) of 1 – **5**.
[c]Measurements were made at 1/R = [Cu]/[NP] value of 1 for complexes **2** – **5**, concentration of DNA = $5 \times 10^{-5}$ M. Cell path length, 1 cm.

**Table 4.** Stern-Volmer quenching constants for the interaction of **1 - 5** with BSA[a]

| Complex | $K_{sv} \times 10^4\ M^{-1}$ |
|---|---|
| [Cu(bimda)(bpy)] **1** | 5.3 ± 0.7 |
| [Cu(bimda)(phen)] **2** | 8.2 ± 1.2 |
| [Cu(bimda)(5,6-dmp)] **3** | 10.2 ± 2.0 |
| [Cu(bimda)(3,4,7,8-tmp)] **4** | 18.0 ± 2.5 |
| [Cu(bimda)(dpq)] **5** | 8.4 ± 1.6 |

[a][BSA] = 5 μM; increasing concentration (0 - 50 μM) of **1 – 5**

**Table 5.** *In vitro* cytotoxicity assay for complexes **2** – **5** against MCF-7 breast cancer cell line. [a]$IC_{50}$ values are in μM. (Data are Mean ± SD of three replicates each)

| Complexes | $IC_{50}$, μM | |
|---|---|---|
| | 24 h | 48 h |
| [Cu(bimda)(phen)] **2** | 13.4 ± 1.8 | 11.3 ± 0.5 |
| [Cu(bimda)(5,6-dmp)] **3** | 5.2 ± 0.6 | 4.1 ± 0.6 |
| [Cu(bimda)(3,4,7,8-tmp)] **4** | 3.4 ± 0.4 | 2.5 ± 0.3 |
| [Cu(bimda)(dpq)] **5** | 9.2 ± 0.7 | 7.1 ± 0.6 |
| cisplatin | 26.7 ± 2.2 | 24.5 ± 1.9 |

[a]$IC_{50}$ = concentration of drug required to inhibit growth of 50% of the cancer cells (in μM)

## Research Highlights

The mixed-ligand copper(II) dicarboxylate complexes exhibit cytotoxicity against human breast cancer cell lines with potency more than cisplatin and induce apoptosis.

## Graphical Abstract

The 5,6-dmp and 3,4,7,8-tmp complexes exhibit strong DNA and protein binding affinity, display prominent double-strand DNA cleavage and also exhibit a cytotoxicity more prominent than others due to the enhanced hydrophobicity of 5,6-dmp, 3,4,7,8-tmp co-ligands, which facilitate the transport of the complexes across cell membrane and thus induce apoptosis.

## Graphical Figure

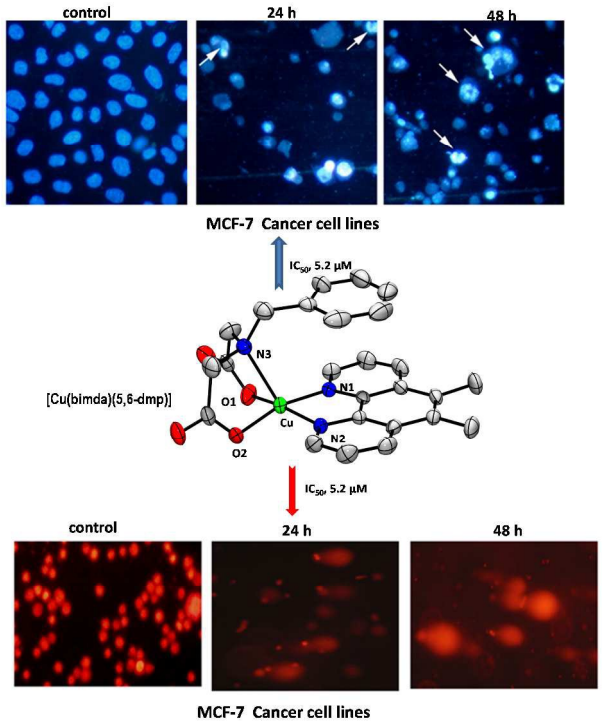

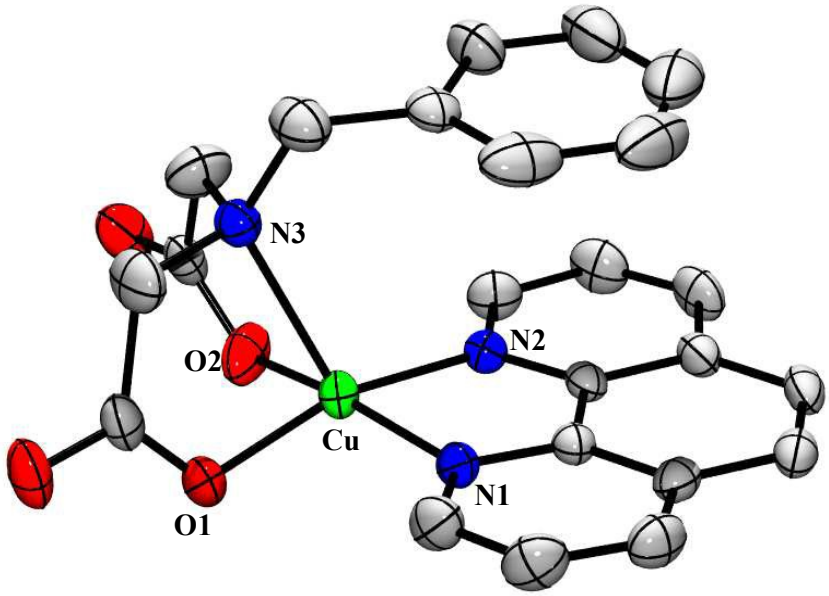


**Figure 1.** ORTEP view of [Cu(bimda)(phen)] (**2**) showing atom numbering scheme and displacement ellipsoids (50% probability level). Hydrogen atoms are omitted for clarity

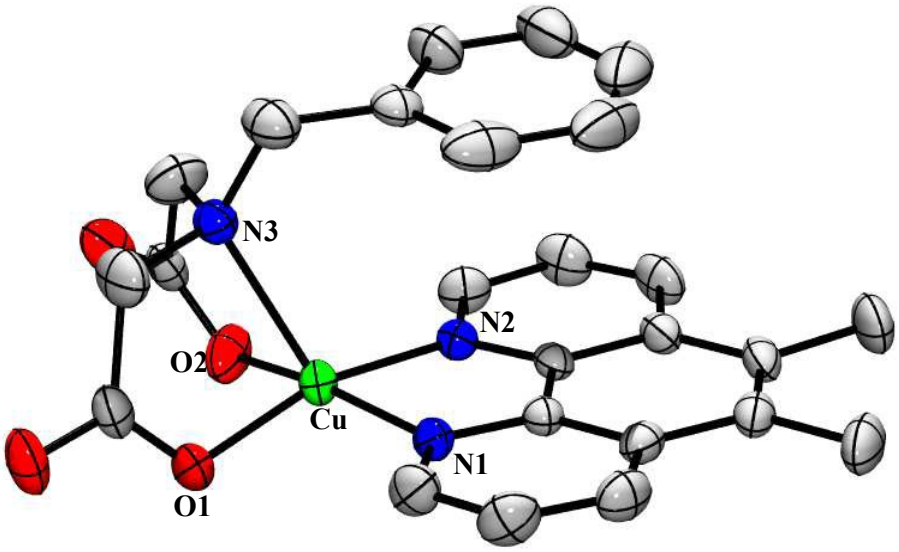


**Figure 2.** ORTEP view of [Cu(bimda)(5,6-dmp)] (**3**) showing atom numbering scheme and displacement ellipsoids (50% probability level). Hydrogen atoms are omitted for clarity

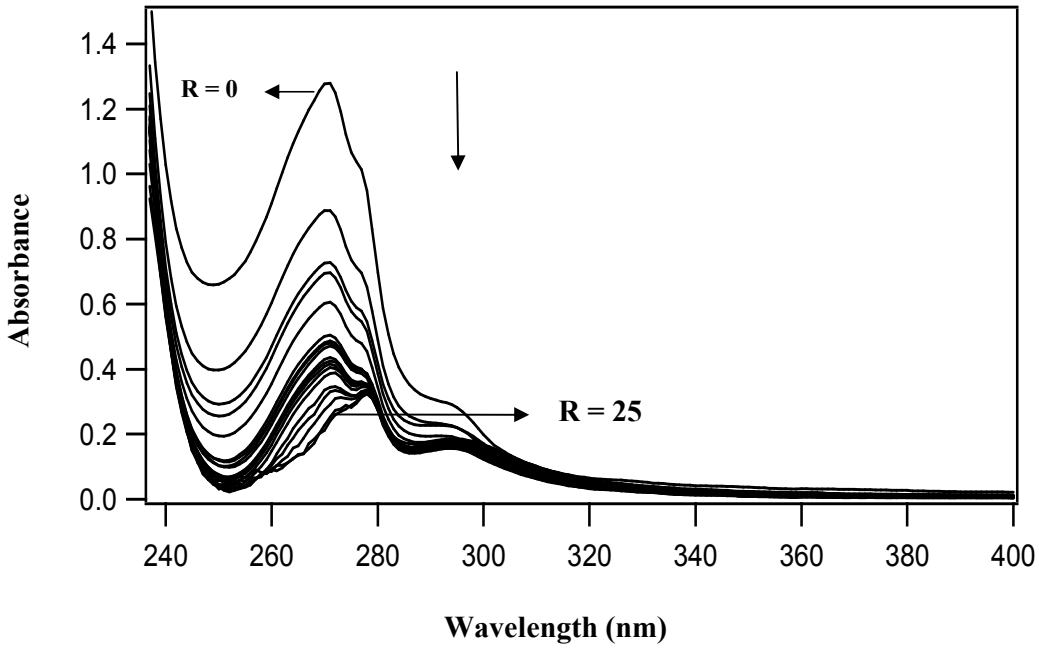


**Figure 3.** Absorption spectra of [Cu(bimda)(phen)] in 5 mM Tris HCl/50 mM NaCl in the absence and presence of increasing amount of CT DNA

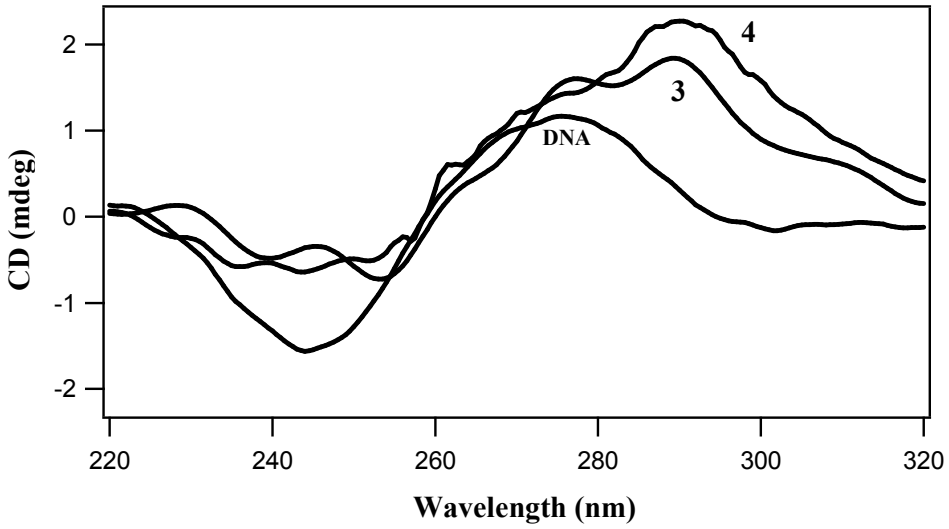


**Figure 4.** Circular dichroism spectra of CT DNA ($4 \times 10^{-4}$ M) in 5 mM Tris-HCl/50 mM NaCl buffer at pH 7.1 and 25 $^{o}$C in the absence (DNA) and presence of [Cu(bimda)(5,6-dmp)] (**3**) and [Cu(bimda)(3,4,7,8-tmp)] (**4**) at 1/R value of 1.

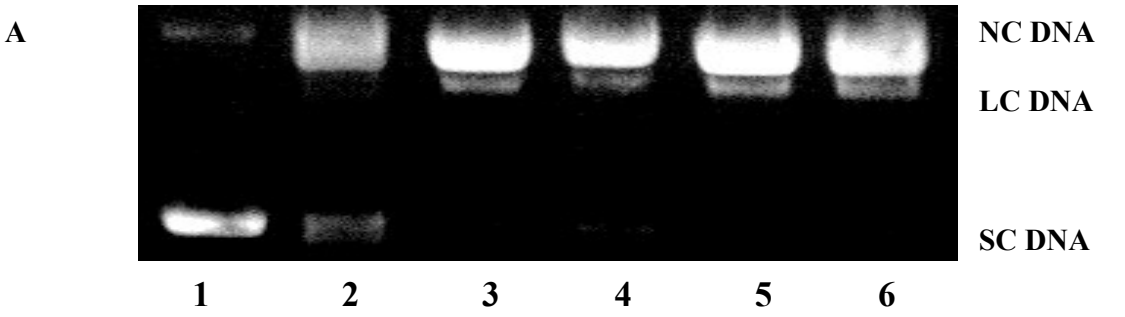


**Figure 5A.** The cleavage of supercoiled pUC19 DNA (40 μM) by complexes **1 – 5** (100 μM) with incubation time of 1 h in 5 mM Tris-HCl/50 mM NaCl buffer at pH 7.1. Lane 1, DNA control; Lane 2, DNA + **1**; Lane 3, DNA + **2**; Lane 4, DNA + **3**; Lane 5, DNA + **4;** Lane 6, DNA + **5**. Forms SC, NC and LC are Supercoiled, Nicked Circular and Linear Circular DNA respectively

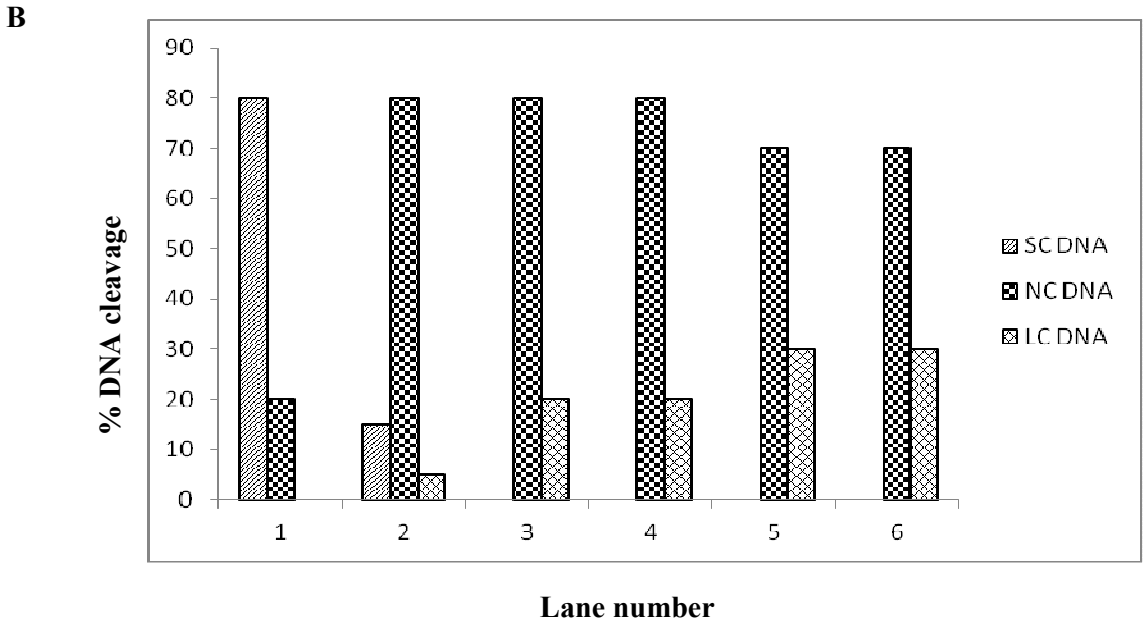


**Figure 5B.** Plot shows % DNA cleavage *vs.* complexes **1** - **5** (100 μM) for an incubation period of 1 h

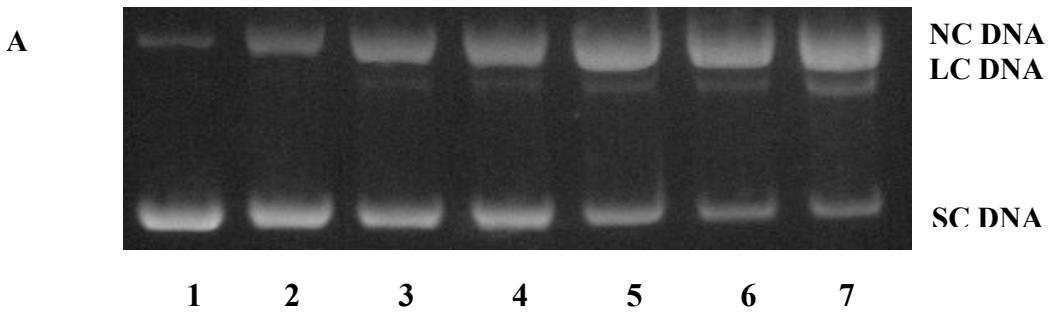


**Figure 6A.** Concentration dependent cleavage of SC pUC19 DNA (40 μM in base pair) with different concentration of complex **5**. Lane 1, DNA; lane 2, DNA + **5** (20 μM); lane 3, DNA + **5** (40 μM); lane 4, DNA + **5** (60 μM); lane 5, DNA + **5** (80 μM); lane 6, DNA + **5** (100 μM); lane 7, DNA + **5** (120 μM). Forms SC, NC and LC are Supercoiled, Nicked Circular and Linear Circular DNA respectively

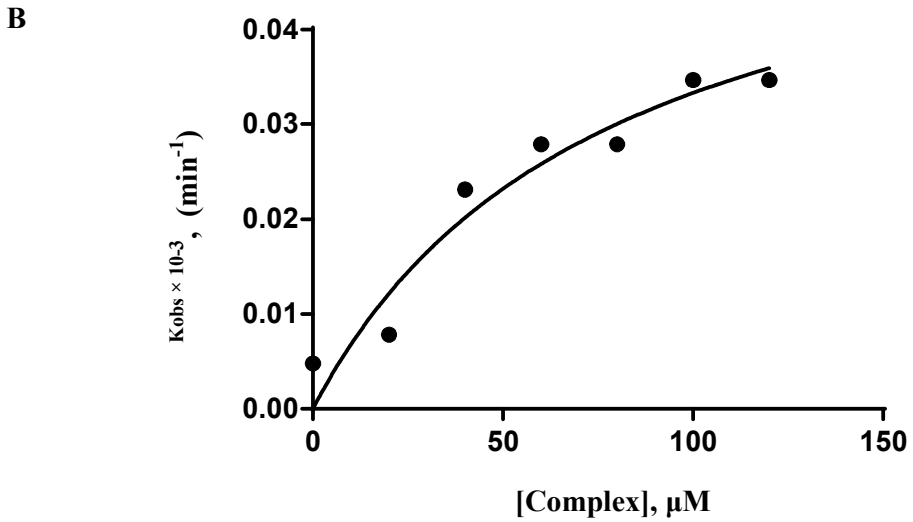


**Figure 6B.** Plot shows pseudo-Michaelis-Menten Kinetics of the cleavage of SC pUC19 DNA with different complex concentrations of **5** (20 – 120 μM) for 1 h

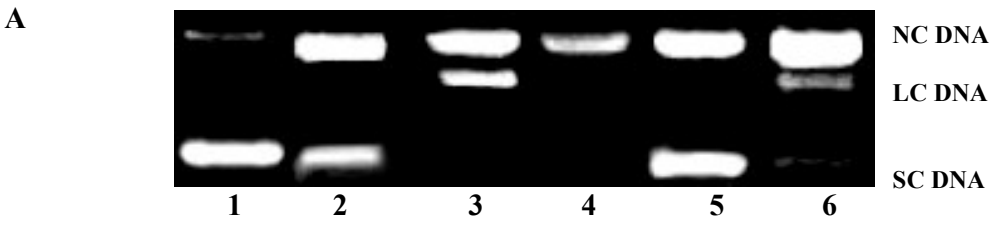


**Figure 7A.** Gel electrophoresis diagram of cleavage of supercoiled pUC19 DNA (40 μM) by the complex **5** (100 μM) in 5 mM Tris-HCl/50 mM NaCl at pH = 7.1 and in the presence of different additives at 37 $^{o}$C. Lane 1, DNA; Lane 2, DNA + **5** + catalase (10 unit); Lane 3, DNA + **5** + $NaN_3$ (100 μM); Lane 4, DNA + **5** + SOD (4 unit); Lane 5, DNA + **5** + DMSO (6 μL); Lane 6, DNA + **5**. Forms SC, NC and LC are Supercoiled, Nicked Circular and Linear Circular DNA respectively

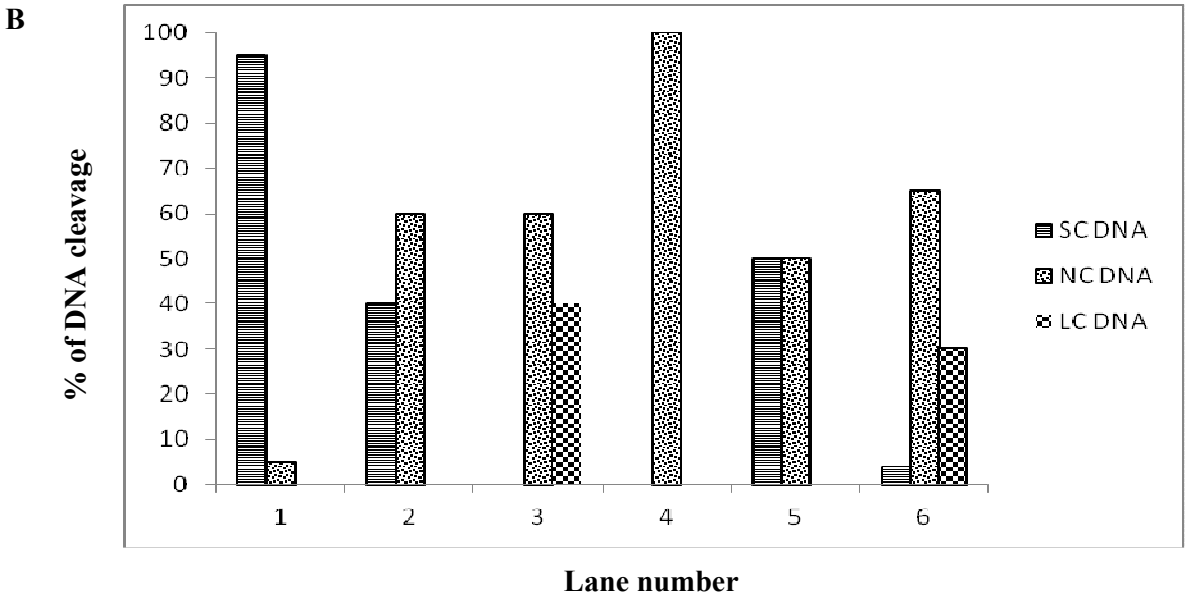


**Figure 7B.** Bar diagram showing the relative amounts of the different DNA forms in the presence of complex **5** and different additives

A

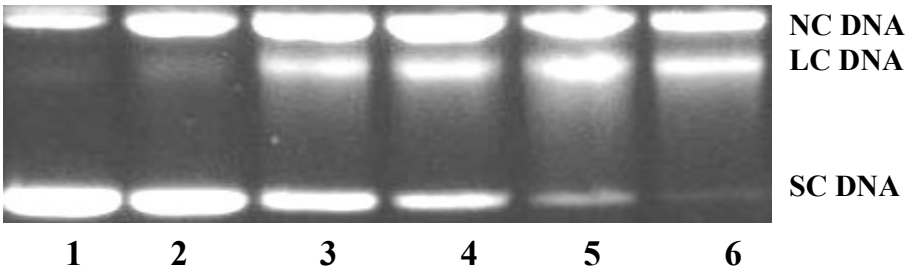


**Figure 8A.** Cleavage of supercoiled pUC19 DNA (40 μM) by copper(II) complexes in a buffer containing 5 mM Tris HCl and 50 mM NaCl in the presence of ascorbic acid ($H_2A$, 10 μM) at 37 $^oC$. Lane 1, DNA + $H_2A$; Lane 2, DNA + $H_2A$ + **1**; Lane 3, DNA + $H_2A$ + **2**; Lane 4, DNA + $H_2A$ + **3**; Lane 5, DNA + $H_2A$ + **4**; Lane 6, DNA + $H_2A$ + **5.** Complex concentration is 30 μM for lanes 2 - 6

B

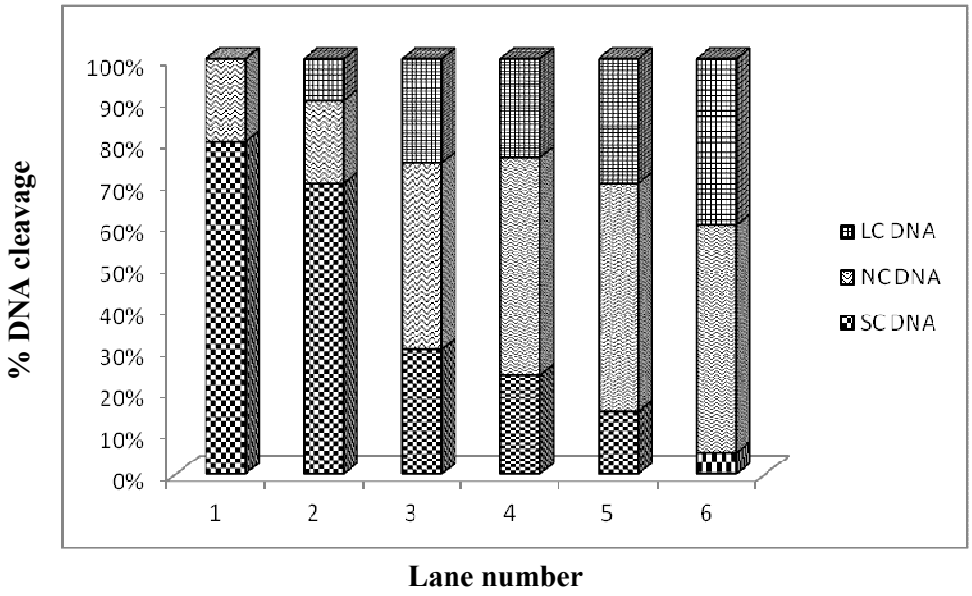


**Figure 8B.** Plot shows % DNA cleavage vs. complexes **1** - **5** (30 μM) for an incubation period of 1 h

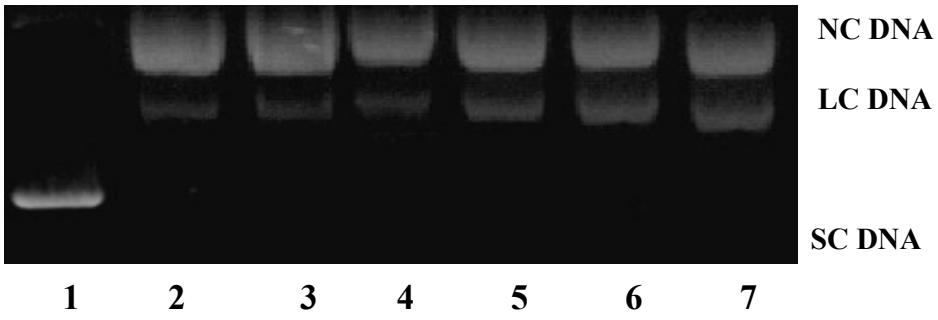


**Figure 9.** Cleavage of supercoiled pUC19 DNA (40 μM) by copper(II) complexes in a buffer containing 5 mM Tris HCl and 50 mM NaCl in the presence of ascorbic acid ($H_2A$, 10 μM) at 37 $^oC$. Lane 1, DNA + $H_2A$; Lane 2, DNA + $H_2A$ + **5** (5 μM); Lane 3, DNA + $H_2A$ + **5** (10 μM); Lane 4, DNA + $H_2A$ + **5** (15 μM); Lane 5, DNA + $H_2A$ + **5** (20 μM); Lane 6, DNA + $H_2A$ + **5** (25 μM); Lane 7, DNA + $H_2A$ + **5** (30 μM)

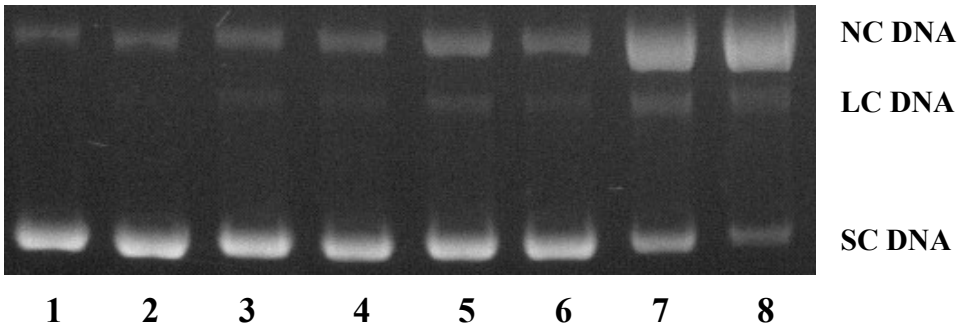


**Figure 10.** Cleavage of supercoiled pUC19 DNA (40 μM) by copper(II) complexes in a buffer containing 5 mM Tris HCl and 50 mM NaCl in the presence of ascorbic acid ($H_2A$, 10 μM) at 37 $^oC$. Lane 1, DNA control; Lane 2, DNA + $H_2A$; Lane 3, DNA + $H_2A$ + **4** (5 μM); Lane 4, DNA + $H_2A$ + **4** (10 μM); Lane 5, DNA + $H_2A$ + **4** (15 μM); Lane 6, DNA + $H_2A$ + **4** (20 μM); Lane 7, DNA + $H_2A$ + **4** (25 μM); Lane 8, DNA + $H_2A$ + **4** (30 μM)

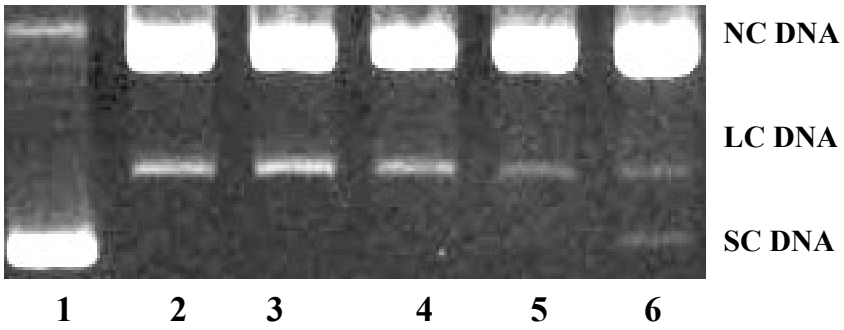


**Figure 11.** Gel electrophoresis diagram of cleavage of supercoiled pUC19 DNA (40 μM) by the complex **5** (30 μM) in the presence of ascorbic acid ($H_2A$) in 5 mM Tris-HCl/50 mM NaCl at pH = 7.1 and in the presence of different additives at 37 $^oC$. Lane 1, DNA + **5;** Lane 2, DNA + **5** + $H_2A$; Lane 3, DNA + **5** + $H_2A$ + $NaN_3$ (100 μM) ; Lane 4, DNA + **5** + $H_2A$ + SOD (4 unit); Lane 5, DNA + **5** + $H_2A$ + catalase (10 unit); Lane 6, DNA + **5** + $H_2A$ + DMSO (6 μL). Forms SC, NC and LC are Supercoiled, Nicked Circular and Linear Circular DNA respectively

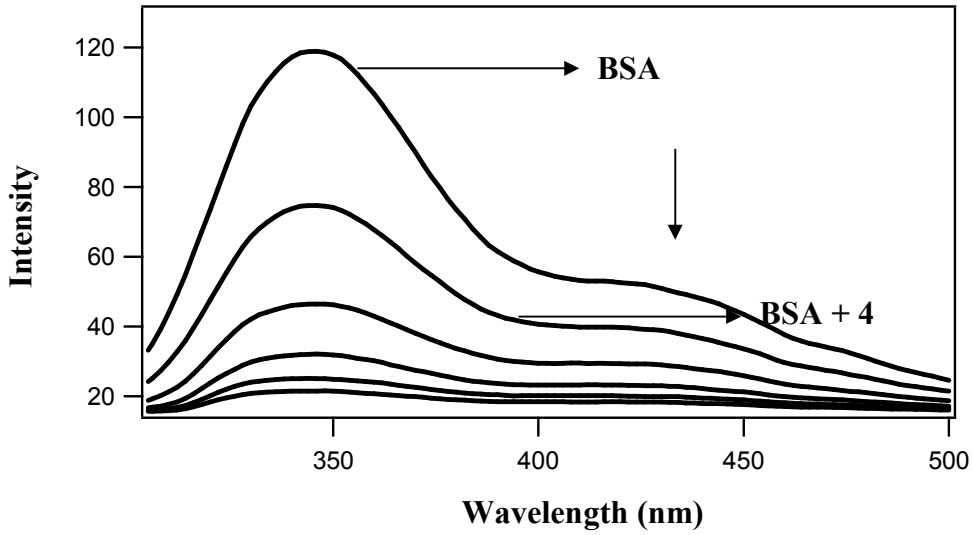


**Figure 12.** Fluorescence quenching of BSA in the absence and presence of **4** in phosphate buffer at pH 7.1. Excitation wavelength, 295 nm

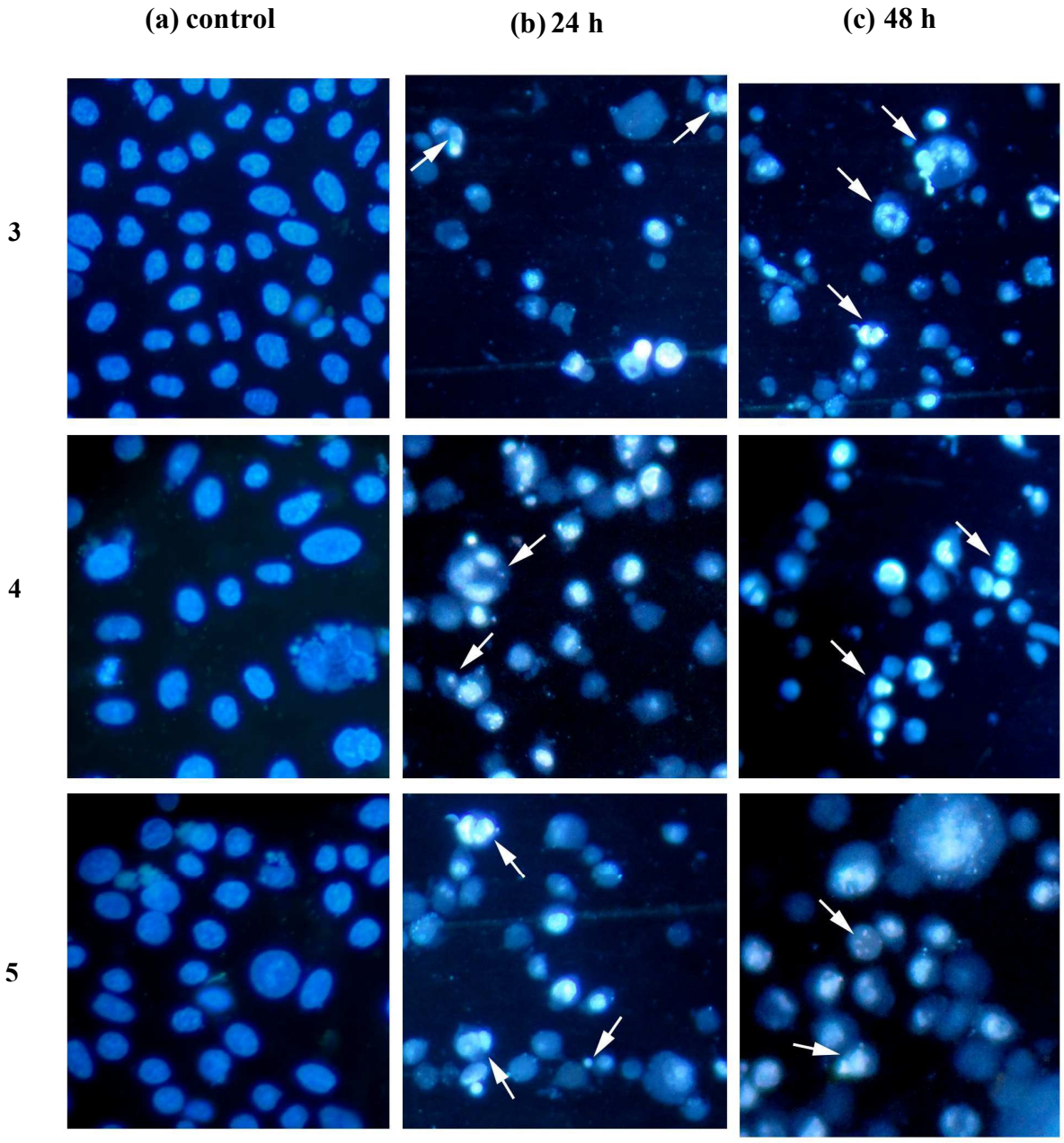


**Figure 13.** Photomicrograph showing the features of Hoechst 33258 staining of MCF-7 breast cancer cells. Cancer cells were treated with $IC_{50}$ concentrations of **3 - 5**. The cells were stained with Hoechst 33258 fluorescent dye: (a) untreated MCF-7 breast cancer cells (control), (b) MCF-7 breast cancer cells treated with **3 - 5** after 24 h seeding, (c) MCF-7 breast cancer cells treated with **3 - 5** after 48 h seeding; Apoptotic body formation is indicated by arrows.

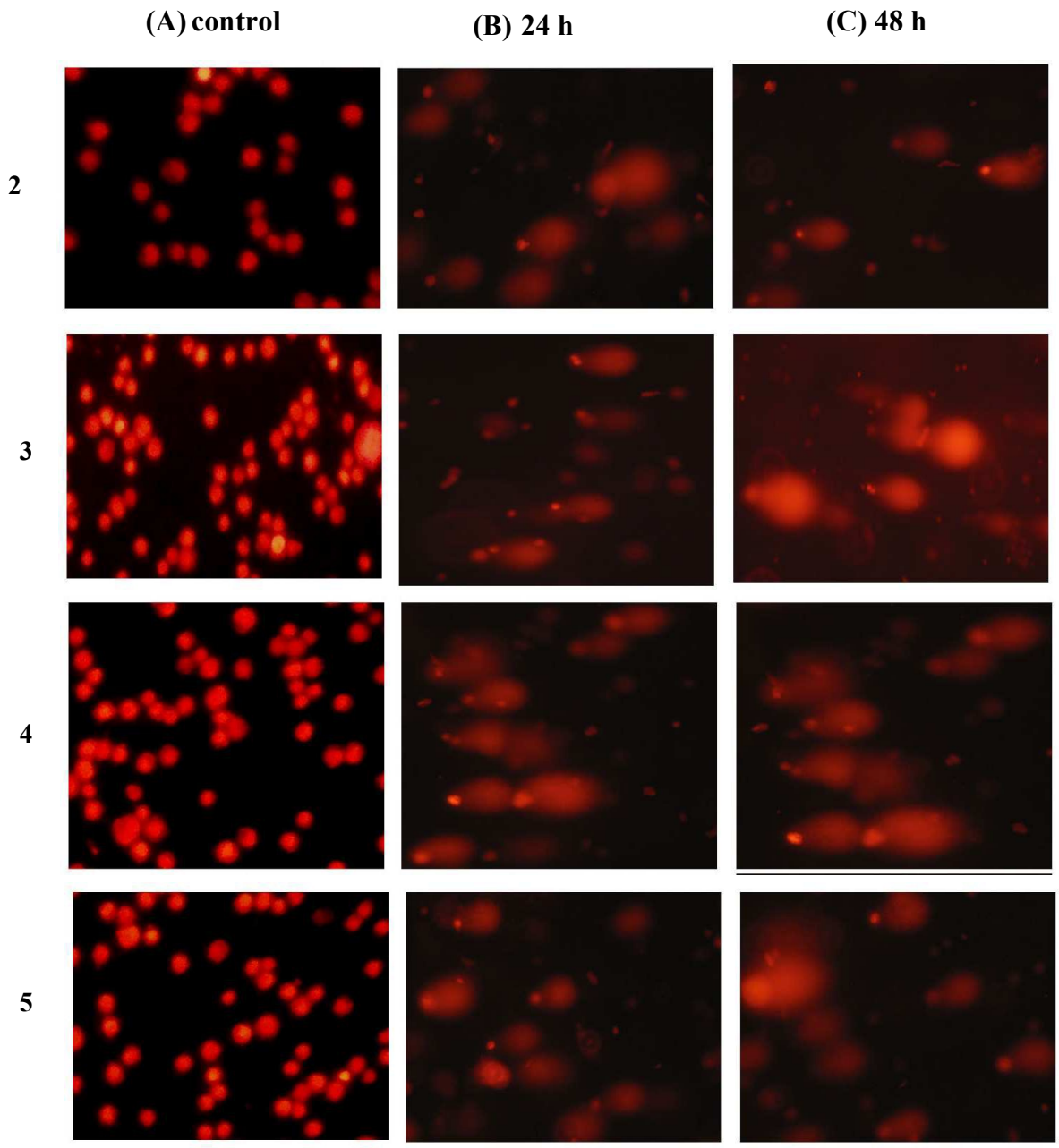


**Figure 14.** Comet assay of EthBr-stained of MCF-7 breast cancer cells. (a) MCF-7 breast cancer cells (untreated), (b) MCF-7 breast cancer cells treated with $IC_{50}$ concentrations of **2** - **5** at 24 h incubation, (c) at 48 h incubation